

Diffraction by a Dirichlet right angle on a discrete planar lattice

A. V. Shanin, A. I. Korolkov

September 9, 2020

Abstract

A problem of scattering by a Dirichlet right angle on a discrete square lattice is studied. The waves are governed by a discrete Helmholtz equation. The solution is looked for in the form of the Sommerfeld integral. The Sommerfeld transformant of the field is built as an algebraic function. The paper is a continuation of [1].

NOTATIONS

$\mathbb{C}, \bar{\mathbb{C}}$	complex plane and Riemann sphere
K	wavenumber parameter of equation (1)
$u(m, n)$	wave field on the lattice
ϕ_{in}, ϕ	angle of propagation of the incident wave, angle of scattering
m, n	indexes of nodes in the discrete physical plane
x, y	wavenumber parameters
\mathbf{S}_3	branched discrete plane, introduced in [1]
$w_{m,n}(x, y)$	plane wave (3)
$x_{\text{in}}, y_{\text{in}}$	wavenumber parameters of the incident wave
$\hat{D}(x, y)$	dispersion function (5)
$\Xi(x)$	root of dispersion equation (8) defined by (10)
$\Upsilon(x)$	irrationality of $\Xi(x)$, (14)
\mathbf{R}	Riemann surface of $\Xi(x)$ or $\Upsilon(x)$
\mathbf{R}_3	a 3-sheet covering of \mathbf{R}
$P_{3:1}, P_{1:0}$	projections between $\mathbf{R}_3, \mathbf{R}_1$, and $\bar{\mathbb{C}}$
\mathbf{D}	dispersion surface
\mathbf{D}_3	a 3-sheet covering of \mathbf{D}
\tilde{x}, \hat{x}, x	notations for points on \mathbf{R}_3, \mathbf{R} , and $\bar{\mathbb{C}}$ linked by natural projections
$\eta_{1,1}, \eta_{1,2}, \eta_{2,1}, \eta_{2,2}$	branch points of \mathbf{R} , defined by (12), (13)
Λ, Π, Π'	symmetries of \mathbf{R}_3 , see (21), (23)
$A(\tilde{x})$	Sommerfeld transformant of the field (see representation (17))
A_0, A_1, A_2	the components of A having different properties with respect to Λ
$\tilde{x}_1, \tilde{x}_2, \tilde{x}_3, \tilde{x}_4$	prescribed poles of A on \mathbf{R}_3
Y_1, \dots, Y_4	residues of A
$w_{m,n}(x, y)$	discrete plane wave, (7)
Γ_2, Γ_3	contours for the Sommerfeld integral
$J_2, J_3, J'_1, J'_3, J'_4$	contours encircling zero / infinity points on \mathbf{R}_3
$\mathbf{K}_0, \mathbf{K}_1, \mathbf{K}_3$	fields of functions meromorphic on $\bar{\mathbb{C}}$, on \mathbf{R} , and on \mathbf{R}_3 , respectively
$\Omega_{j:l}$	basis of extension \mathbf{K}_j over \mathbf{K}_l
$F_1(x), F_2(x)$	nontrivial elements of the basis $\Omega_{3:1}$
ϖ	$\exp\{2\pi i/3\}$, cubic root of 1
$\hat{\mathbf{b}}, \mathbf{b}$	an important point on \mathbf{R} used for building F_1 and its affix
$\chi(\hat{x}), T_\alpha, T_\beta$	Abelian integral of the first kind on \mathbf{R} (see (46)) and its periods
α, β	natural coordinates on the torus \mathbf{R}
ψ	mapping $\chi \rightarrow \hat{x}$

1 Introduction

This paper continues the research presented in [1]. A 2D discrete square lattice is under consideration. The lattice bears a discrete Helmholtz equation with a 5-point stencil. The first quadrant of the lattice is blocked by setting the field equal to zero there. The problem of diffraction of an incident plane wave by the blocked angle is studied. The motivation and the literature review for such a problem can be found in [1].

A new formalism has been developed for this problem. Similarly to continuous problems of diffraction in angular domains, a branching surface \mathbf{S}_3 is introduced in the physical discrete plane, and the diffraction problem is reformulated as a propagation problem on this surface by using the reflection principle. An analog of the Sommerfeld integral for field representation is introduced. This integral is a contour integral on a complex manifold \mathbf{D} that is the dispersion diagram for waves on the discrete plane. Topologically, this dispersion diagram is a torus. The integrand is a differential form that is multivalued on the dispersion diagram and possesses prescribed poles corresponding to the incident wave and reflected waves. The contour of integration depends on the position of the observation point, and “slides” along the surface as the observation point moves.

The integrand form contains an unknown function referred to as the Sommerfeld transformant of the field. It obeys a certain functional problem. In [1] the authors found this transformant in terms of elliptic functions. However, such a representation is not convenient. Moreover, it can be proven that such a transformant should be an algebraic function, thus, a representation through the elliptic functions is somewhat unnecessarily complicated. The aim of the current paper is to build the Sommerfeld transformant of the field as an algebraic function, and then to study the properties of the field.

The paper is organized as follows. In Section 2 the initial diffraction problem is formulated. Then, the main result of [1] in application to the angle diffraction problem is written down. Namely, a functional problem for the Sommerfeld transformant is set. In Section 3 the process of finding the transformant is outlined. Namely, it is proposed first to find the functional field \mathbf{K}_3 to which the transformant belongs, and then to specify the transformant in this field. The field is presented by its basis, and the particular element in it is constructed as a linear combination of the basis elements. In Section 4 the basis of the field \mathbf{K}_3 is constructed. This is the most tricky part of the paper. In Section 5 the coefficients of representation of the Sommerfeld transformant through the basis of the field are found. Thus, the representation of the wave field in the form of the Sommerfeld integral becomes obtained. In Section 6 the constructed field representation is carefully checked. We demonstrate that the result obeys all condition imposed by the initial diffraction problem. This section can be considered as a double check of the argument of [1] used for developing of the Sommerfeld integral formalism. In Section 7 some numerical checks are performed. We demonstrate the process of building the basis function and, finally, compute the solution of the diffraction problem.

2 Problem formulation

Consider a planar square lattice whose nodes have integer indices (m, n) . Let the homogeneous discrete Helmholtz equation

$$u(m, n - 1) + u(m, n + 1) + u(m - 1, n) + u(m + 1, n) + (K^2 - 4)u(m, n) = 0 \quad (1)$$

be valid in the domain

$$m < 0 \quad \text{or} \quad n < 0$$

(see Fig. 1). The wavenumber parameter K has a positive real part and a small positive imaginary part corresponding to an energy absorption.

The set of nodes with

$$(m = 0 \text{ and } n \geq 0) \text{ or } (n = 0 \text{ and } m \geq 0)$$

is the boundary of the domain. We assume that this boundary is of the Dirichlet type, so

$$u(m, n) = 0 \quad (2)$$

on it.

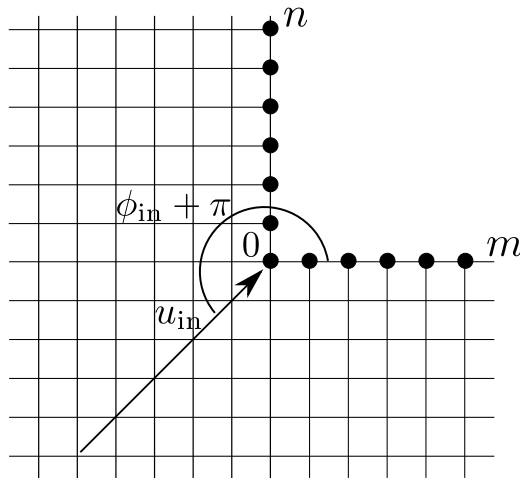


Fig. 1: Geometry of the problem of diffraction by an angle. Black circles show the position of the Dirichlet boundary (blocked nodes)

The total wave is a sum of the incident wave and the scattered wave:

$$u(m, n) = u_{\text{in}}(m, n) + u_{\text{sc}}(m, n),$$

where

$$u_{\text{in}}(m, n) = x_{\text{in}}^m y_{\text{in}}^n, \quad (3)$$

where x_{in} and y_{in} are wavenumber parameters. These parameters obey the dispersion equation:

$$\hat{D}(x_{\text{in}}, y_{\text{in}}) = 0, \quad (4)$$

$$\hat{D}(x, y) \equiv x + x^{-1} + y + y^{-1} + K^2 - 4. \quad (5)$$

We assume that the wave travels into the direction of positive m and n . This means that

$$|x_{\text{in}}| < 1, \quad |y_{\text{in}}| < 1.$$

Besides, we can introduce the angle of incidence by the relation

$$\phi_{\text{in}} \equiv \arctan \left(\frac{y - y^{-1}}{x - x^{-1}} \right). \quad (6)$$

We assume that angle ϕ_{in} is real, and

$$0 < \phi_{\text{in}} < \pi/2.$$

The scattered wave u_{sc} should obey the radiation condition, i. e. it should decay at infinity. The aim is to find u_{sc} .

2.1 The main result of [1]

In [1] the authors developed the Sommerfeld integral technique for the lattice diffraction problem formulated above. The unknown function describing the field is the Sommerfeld transformant. The problem for finding the Sommerfeld transformant is formulated as a problem of finding a meromorphic function of a certain Riemann surface. The transformant should have prescribed poles and residues.

Plane waves on the lattice have form

$$w_{m,n} = w_{m,n}(x, y) = x^m y^n, \quad (7)$$

provided that the pair of wavenumber parameters (x, y) obey the dispersion equation

$$\hat{D}(x, y) = 0. \quad (8)$$

One can see that (8) guarantees fulfillment of the homogeneous Helmholtz equation (1) by w .

The set of all complex pairs $(x, y) \in \mathbb{C}^2$ obeying (8) is referred to as the dispersion diagram of the lattice. Denote this set by \mathbf{D} . This is a complex manifold¹ embedded in \mathbb{C}^2 . The simplest way to represent \mathbf{D} is to express y as a function of x using (8):

$$y(x) = \Xi(x) \quad \text{or} \quad y(x) = \Xi^{-1}(x), \quad (9)$$

¹ A complex manifold [2] is a union of possibly intersecting neighborhoods in each of which a local complex variable can be introduced, describing the neighborhood in a trivial way. The transition between the local variables in intersecting neighborhoods is holomorphic. We assume also that the coordinates x and y are holomorphic functions of local variables. For \mathbf{D} , one can take x as a local variable everywhere except the neighborhoods of the points $\eta_{j,l}$ (see (12), (13)) and except the neighborhoods of the infinities. In the neighborhoods of the points $\eta_{j,l}$ one can choose y as a local variable. At the infinities one can use x^{-1} .

$$\Xi(x) = -\frac{K^2 - 4 + x + x^{-1}}{2} + \frac{i\sqrt{4 - (K^2 - 4 + x + x^{-1})^2}}{2}, \quad (10)$$

$$\Xi^{-1}(x) = -\frac{K^2 - 4 + x + x^{-1}}{2} - \frac{i\sqrt{4 - (K^2 - 4 + x + x^{-1})^2}}{2}, \quad (11)$$

and study the Riemann surface \mathbf{R} of $\Xi(x)$. This Riemann surface is a projection of the manifold \mathbf{D} onto the coordinate x . Topologically, \mathbf{D} and \mathbf{R} are similar.

The complex structure of \mathbf{D} is pulled to \mathbf{R} by the projection, thus \mathbf{R} is also a complex manifold.

One can see that \mathbf{R} has two sheets over $\overline{\mathbb{C}}$. The branch points of the surface are $\eta_{1,1}$, $\eta_{1,2}$, $\eta_{2,1}$, $\eta_{2,2}$:

$$\eta_{1,1} = -\frac{d}{2} - \frac{i\sqrt{4 - d^2}}{2}, \quad \eta_{2,1} = -\frac{d}{2} + \frac{i\sqrt{4 - d^2}}{2}, \quad d = K^2 - 2, \quad (12)$$

$$\eta_{1,2} = -\frac{d}{2} + \frac{\sqrt{d^2 - 4}}{2}, \quad \eta_{2,2} = -\frac{d}{2} - \frac{\sqrt{d^2 - 4}}{2}, \quad d = K^2 - 6. \quad (13)$$

All branch points are of second order. One can see that $y = \pm 1$ at the branch points.

The scheme of \mathbf{R} is shown in Fig. 2. The branch points are connected by cuts (shown by bold lines). The sides of the cuts marked by the same Roman numbers should be attached to each other. For definiteness, the cuts on \mathbf{R} are conducted in such a way that $|y(x)| = 1$ on them. The Riemann surface \mathbf{R} is compactified, i. e. two infinite points are added to the sheets. These infinite points are not branch points. We select the *physical sheet* (or sheet 1) of \mathbf{R} as the sheet on which $|\Xi(x)| < 1$ on the unit circle $|x| = 1$. The unit circle on the physical sheet is shown by a dashed line in the figure.

Introduce the function

$$\Upsilon(x) = x(\Xi(x) - \Xi^{-1}(x)) = \sqrt{(x - \eta_{1,1})(x - \eta_{1,2})(x - \eta_{2,1})(x - \eta_{2,2})} = \quad (14)$$

$$x\sqrt{(K^2 - 4 + x + x^{-1})^2 - 4},$$

$$\Xi(x) = -\frac{K^2 - 4 + x + x^{-1}}{2} + \frac{\Upsilon(x)}{2x} \quad (15)$$

The first and the second representation in (14) are equivalent (one can check this), but the first one links the the branch of the square root of Υ to that of Ξ . Indeed, $\Upsilon(x)$ is the irrationality of $\Xi(x)$, thus the Riemann surface of $\Upsilon(x)$ is the same as of $\Xi(x)$, i. e. this surface is \mathbf{R} .

Topologically, \mathbf{R} is a torus, and thus \mathbf{D} is a torus as well. This fact has been heavily commented and exploited in [1].

One of the main ideas of [1] is as follows. Application of the reflection principle to the physical configuration shown in Fig. 1 leads to a branched discrete physical plane having three sheets (it is referred to as \mathbf{S}_3 in [1]). To construct a Sommerfeld integral for the field, one needs a three-sheet covering of the dispersion diagram \mathbf{D} . There exist several three-sheet coverings

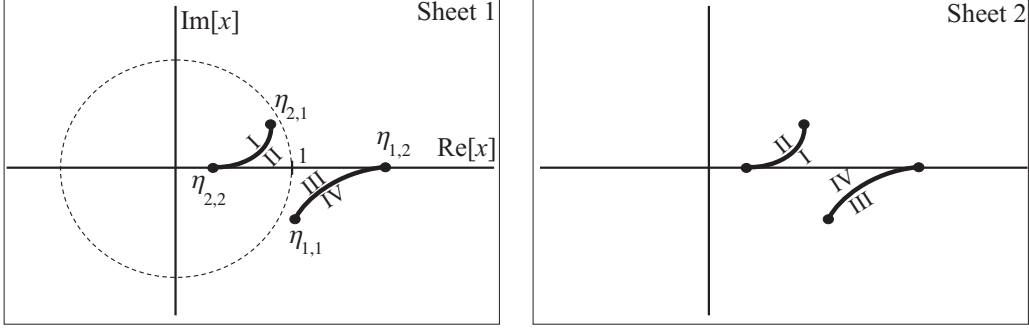


Fig. 2: Riemann surface \mathbf{R}

of \mathbf{D} . One should select the particular covering that triples the “real wave” contour and leaves unchanged the contour of integration for the Green’s function. These two selected contours are homotopic to the loops σ_α and σ_β , respectively, introduced below. Corresponding covering denoted by \mathbf{D}_3 is built in [1] (see Fig. 13 there).

Here we specify the covering \mathbf{D}_3 over \mathbf{D} by its projection onto the variable x . The result is the covering \mathbf{R}_3 over \mathbf{R} . \mathbf{R}_3 is a Riemann surface whose scheme is shown in Fig. 3. Note that there is no function having such a Riemann surface is known *a priori*.

The complex structure of \mathbf{D} remains valid on \mathbf{D}_3 , thus \mathbf{D}_3 is a complex manifold *immersed* in \mathbb{C}^2 . Indeed, topologically \mathbf{D}_3 (or \mathbf{R}_3) is also a torus. The Riemann surface \mathbf{R}_3 is a 3-sheet covering of \mathbf{R} without branching, therefore any function meromorphic on \mathbf{R} is also meromorphic on \mathbf{R}_3 . Sheets 1, 3, and 5 of \mathbf{R}_3 shown in Fig. 3 correspond to the physical sheet of \mathbf{R} .

Introduce notations for the points of the compactified complex plane $\bar{\mathbb{C}}$ of x , and for the Riemann surfaces \mathbf{R} , \mathbf{R}_3 . The points of \mathbf{R}_3 will be indicated by the $\tilde{\cdot}$ decoration, the points of \mathbf{R} will be indicated by the $\hat{\cdot}$ decoration, and the points of $\bar{\mathbb{C}}$ will exist without decorations. For example,

$$\tilde{x} \in \mathbf{R}_3, \quad \hat{x} \in \mathbf{R}, \quad x \in \bar{\mathbb{C}}.$$

There exist natural projections that constitute the definitions of coverings:

$$\tilde{x} \xrightarrow{P_{3:1}} \hat{x} \xrightarrow{P_{1:0}} x.$$

The projections $\tilde{x} \rightarrow x$ and $\hat{x} \rightarrow x$ are taking an *affix* of a point of a Riemann surface.

It is important to notice that we keep the following convention in the whole paper: everywhere \hat{x} is the projection of \tilde{x} , and x is a projection of \hat{x} and \tilde{x} . Indeed, this is valid for any letter instead of x (it may be, say, a or \mathbf{b}). This can be written as

$$\hat{\cdot} \equiv P_{3:1}(\tilde{\cdot}), \quad \cdot \equiv P_{1:0}(\hat{\cdot}) \equiv P_{1:0}(P_{3:1}(\tilde{\cdot})), \quad (16)$$

where \cdot stays for any letter, possibly with indexes, but without a decoration.

If function $f(\hat{x})$ is single valued on \mathbf{R} , there is no difficulty to define it on \mathbf{R}_3 as a single-valued function

$$f(\tilde{x}) = f(P_{3:1}(\tilde{x})) = P(\hat{x}).$$

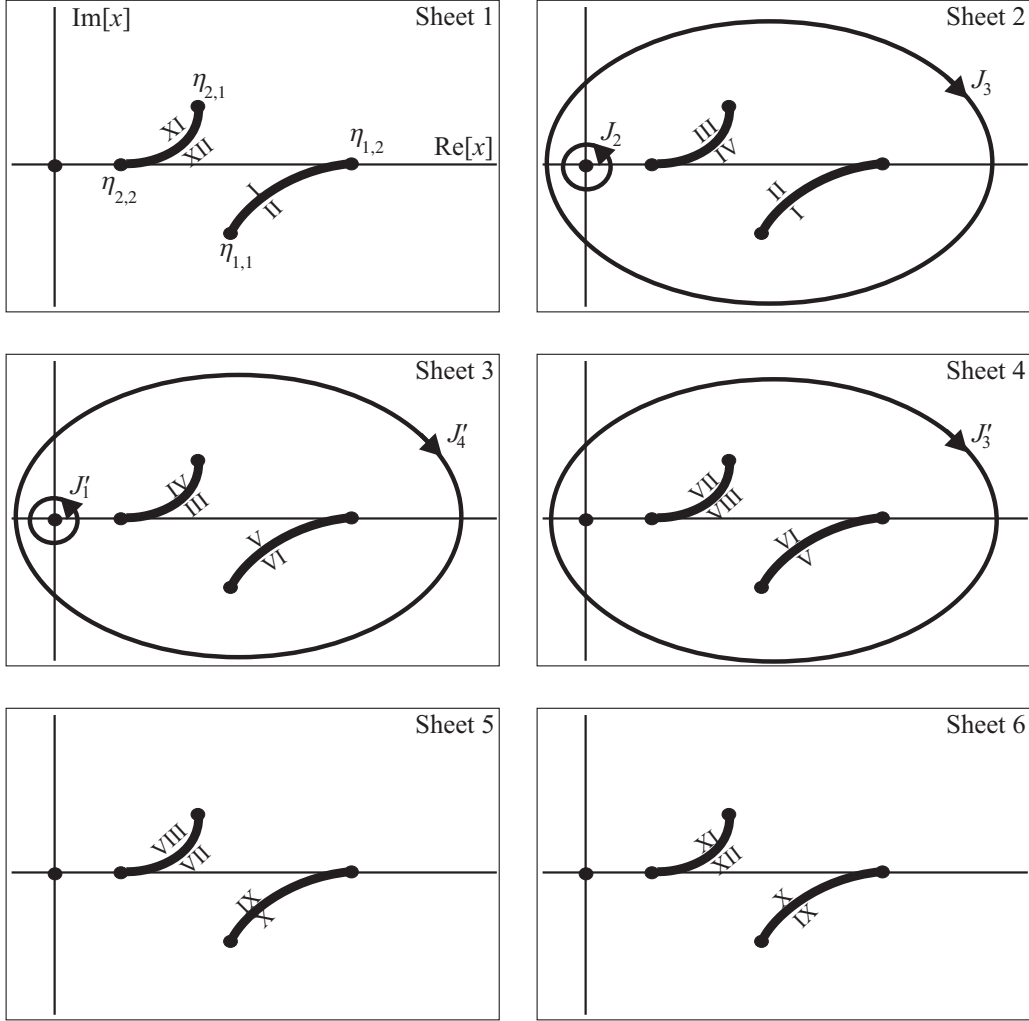


Fig. 3: Riemann surface \mathbf{R}_3 and integration contours on it

Conversely, if $f(\tilde{x})$ is single-valued on \mathbf{R}_3 , the function $f(\hat{x})$ is generally three-valued on \mathbf{R} , and $f(x)$ is six-valued on $\bar{\mathbb{C}}$. Functions $\Upsilon(\hat{x})$ and $\Xi(\hat{x})$ are single-valued; functions $\Upsilon(x)$ and $\Xi(x)$ are two-valued.

Let $\tilde{x}_1, \dots, \tilde{x}_4$ be the points of \mathbf{R}_3 which are specified by the affixes x_j , the values $y = y(\tilde{x})$ and the sheets of \mathbf{R}_3 to which they belong:

$$\begin{aligned} \tilde{x}_1 &: (x_{\text{in}}, y_{\text{in}}), \text{ sheet 3}, & \tilde{x}_2 &: (x_{\text{in}}, y_{\text{in}}^{-1}), \text{ sheet 4}, \\ \tilde{x}_3 &: (x_{\text{in}}^{-1}, y_{\text{in}}^{-1}), \text{ sheet 6}, & \tilde{x}_4 &: (x_{\text{in}}^{-1}, y_{\text{in}}), \text{ sheet 1}. \end{aligned}$$

As it is shown in [1], the point \tilde{x}_1 corresponds to the incident plane wave, the points \tilde{x}_2 and \tilde{x}_3 correspond to the plane waves reflected by the horizontal and the vertical parts of the boundary, and the point \tilde{x}_4 corresponds to the mirror image of the reflected wave.

Let be

$$Y_j = \Upsilon(\hat{x}_j), \quad j = 1, \dots, 4.$$

One can see that $Y_2 = -Y_1$, $Y_4 = -Y_3$.

Following [1], let us formulate the **functional problem for the Sommerfeld transformant $A(\tilde{x})$ of the wave $u(m, n)$** :

1. $A(\tilde{x})$ is meromorphic on \mathbf{R}_3 . As it follows from this condition, the branch points of $A(x)$ can be located only at $\eta_{1,1}$, $\eta_{1,2}$, $\eta_{2,1}$, $\eta_{2,2}$.
2. Function $A(\tilde{x})$ are regular as $|x| \rightarrow \infty$ on each of the six sheets of \mathbf{R}_3 .
3. Function $A(\tilde{x})$ has four poles on \mathbf{R}_3 . The position of the poles and the residues at them are listed in the following table:

\tilde{x}	x	$y(x)$	Sheet	Residue
\tilde{x}_1	x_{in}	y_{in}	3	$-(2\pi i)^{-1}Y_1$
\tilde{x}_2	x_{in}	y_{in}^{-1}	4	$-(2\pi i)^{-1}Y_1$
\tilde{x}_3	x_{in}^{-1}	y_{in}^{-1}	6	$-(2\pi i)^{-1}Y_3$
\tilde{x}_4	x_{in}^{-1}	y_{in}	1	$-(2\pi i)^{-1}Y_3$

Indeed, once function $A(\tilde{x})$ is found, one can say that \mathbf{R}_3 is the Riemann surface of $A(x)$. Besides, being defined on \mathbf{R}_3 , the function A can be pulled back to \mathbf{D}_3 . So one can consider function A as being a 3-valued function defined on the dispersion diagram of the discrete plane.

Function A , formally, has been found in [1] (see (70) there), however it has been expressed in elliptic functions, and this solution is hardly practical. However, the formulation of the problem is of algebraic nature, so one can expect a purely algebraic solution.

Once $A(\tilde{x})$ is found, the wave field can be built using the Sommerfeld integral introduced in [1] and having the form

$$u(m, n) = \int_{\Gamma_j} w_{m,n}(\hat{x}, \Xi(\hat{x})) A(\tilde{x}) \frac{dx}{\Upsilon(\hat{x})}. \quad (17)$$

The contours of integration Γ_j are drawn on \mathbf{R}_3 . The indexing of the contours is kept similar to that of [1]. For $m \leq 0$ one should select contour Γ_2 :

$$\Gamma_2 = J_3 + J_2 + J'_1 + J'_4. \quad (18)$$

For $n \leq 0$ one should select contour Γ_3 :

$$\Gamma_3 = J_2 + J'_1 + J'_4 + J'_3. \quad (19)$$

The contours J_3 , J_2 , J'_1 , J'_4 , J'_3 are shown in Fig. 3. Contours J_2 and J'_1 encircle the point $x = 0$ on corresponding sheets. Contours J_3 , J'_4 , J'_3 encircle the infinities on corresponding sheets (i. e. they encircle all finite singularities).

The domain with $m \leq 0$ and $n \leq 0$ can be described either by the contour Γ_2 or contour Γ_3 . It is demonstrated in [1] that these representations are equivalent.

In Section 6, to make a trustful presentation, we prove that the field (17) obeys all condition imposed on the solution of the diffraction problem.

The aim of the current paper is to construct the function $A(\tilde{x})$ obeying the properties 1–3 listed above.

3 Mathematical basics of building the Sommerfeld transformant $A(x)$

3.1 Symmetries of the Riemann surface

Let $\tilde{x}^{(j)}$, $j \in \{1, \dots, 6\}$ denote a point of \mathbf{R}_3 having affix x and lying on the sheet number j (the numbering of the sheets is kept as in Fig. 3).

Consider the cyclical change of sheets

$$1 \rightarrow 3 \rightarrow 5 \rightarrow 1, \quad 2 \rightarrow 4 \rightarrow 6 \rightarrow 2. \quad (20)$$

This change generates a symmetry (referred to as Λ) of \mathbf{R}_3 , Namely,

$$\Lambda(\tilde{x}^{(j)}) = \tilde{x}^{(j')}, \quad (21)$$

where the point $\tilde{x}^{(j')}$ has the same affix as $\tilde{x}^{(j)}$, and the sheet j' is obtained from j by applying the function (20).

One can see that if a function $f(\tilde{x})$ is meromorphic on \mathbf{R}_3 then the same is valid for $f(\Lambda(\tilde{x}))$. Moreover, Λ does not change the value of $\Upsilon(\tilde{x})$:

$$\Upsilon(\Lambda(\tilde{x})) = \Upsilon(\tilde{x}). \quad (22)$$

Another symmetry (referred to as Π) is as follows:

$$\Pi(\tilde{x}^{(j)}) = \tilde{x}^{(7-j)} \quad (23)$$

(again, the affix remains the same). One can see that if a function $f(\tilde{x})$ is meromorphic on \mathbf{R}_3 then the same is valid for $f(\Pi(x))$. A direct check shows that

$$\Upsilon(\Pi(\tilde{x})) = -\Upsilon(\tilde{x}). \quad (24)$$

As it is shown in Section 6, the symmetry Π of the Riemann surface \mathbf{R}_3 corresponds to the geometrical symmetry $n \rightarrow -n$ of the initial physical system. The symmetry Π can be elevated to \mathbf{D}_3 . It has form

$$x \rightarrow x, \quad y \rightarrow y^{-1}.$$

The symmetry Λ also has a geometrical interpretation. It corresponds to the change of the sheets of the branched discrete physical plane. Obviously,

$$\Pi(\Pi(\tilde{x})) = \tilde{x}, \quad \Lambda(\Lambda(\Lambda(\tilde{x}))) = \tilde{x}.$$

The symmetries Π and Λ can be used to simplify the formulation of the functional problem for $A(\tilde{x})$. One can see that $A(\tilde{x})$ can be chosen symmetrical:

$$A(\Pi(\tilde{x})) = A(\tilde{x}). \quad (25)$$

since the combination $(A(\tilde{x}) + A(\Pi(\tilde{x}))/2)$ obeys all conditions imposed on A . Besides, one can apply a symmetrization with respect to Λ (i. e. a discrete Fourier transform of dimension 3 for each point \hat{x}), i. e. represent A as the sum of three components

$$A(\tilde{x}) = A_0(\tilde{x}) + A_1(\tilde{x}) + A_2(\tilde{x}), \quad (26)$$

such that

$$A_0(\Lambda(\tilde{x})) = A_0(\tilde{x}), \quad A_1(\Lambda(\tilde{x})) = \varpi A_1(\tilde{x}), \quad A_2(\Lambda(\tilde{x})) = \varpi^{-1} A_2(\tilde{x}), \quad (27)$$

where

$$\varpi \equiv e^{2\pi i/3}. \quad (28)$$

The components of A can be found by the transform

$$A_0(\tilde{x}) = \frac{1}{3} (A(\tilde{x}) + A(\Lambda(\tilde{x})) + A(\Lambda(\Lambda(\tilde{x})))) , \quad (29)$$

$$A_1(\tilde{x}) = \frac{1}{3} (A(\tilde{x}) + \varpi^2 A(\Lambda(\tilde{x})) + \varpi A(\Lambda(\Lambda(\tilde{x})))) , \quad (30)$$

$$A_2(\tilde{x}) = \frac{1}{3} (A(\tilde{x}) + \varpi A(\Lambda(\tilde{x})) + \varpi^2 A(\Lambda(\Lambda(\tilde{x})))) . \quad (31)$$

Each of the functions A_0, A_1, A_2 is meromorphic on \mathbf{R}_3 , is regular at the infinite points, and possesses 12 poles at the points with affixes x_{in} and x_{in}^{-1} . The residues of the poles for each of the functions is given by the following table (common for all three functions):

\tilde{x}	x	Sheet	Residue
\tilde{x}_1	x_{in}	3	$-(6\pi i)^{-1} Y_1$
\tilde{x}_2	x_{in}	4	$-(6\pi i)^{-1} Y_1$
\tilde{x}_3	x_{in}^{-1}	6	$-(6\pi i)^{-1} Y_3$
\tilde{x}_4	x_{in}^{-1}	1	$-(6\pi i)^{-1} Y_3$

Note that the table describes only four poles of twelve. The residues at the other poles of each of the functions can be obtained from (27). Below we solve the functional problems for A_0 , A_1 , A_2 rather than that of for A .

Remark

There is another symmetry Π' of the Riemann surface \mathbf{R}_3 . This symmetry will be used once in Section 6. The choice of x as the independent variable is not unique. In a very similar way, one could use y as an independent variable. In this case, $x = \Xi(y)$ is a double-valued function having a Riemann surface \mathbf{R}' . Indeed, \mathbf{R}' is similar to \mathbf{R} . Moreover, \mathbf{R}' is a projection of the same manifold \mathbf{D} onto another variable.

One can define the Riemann surface \mathbf{R}'_3 as a projection of \mathbf{D}_3 onto y . \mathbf{R}'_3 has the same structure as \mathbf{R}_3 , but the independent variable is y .

There exists a symmetry of \mathbf{R}'_3 constructed the same way as Π . Denote it by Π' . This symmetry has form

$$x \rightarrow x^{-1}, \quad y \rightarrow y$$

and corresponds to the symmetry $m \rightarrow -m$ of the physical plane. One can demonstrate that

$$A(\Pi'(\tilde{x})) = A(\tilde{x}).$$

3.2 Functional fields necessary for solving the diffraction problem

The set of functions $f(x)$ meromorphic on $\bar{\mathbb{C}}$ is a *field* ([3], chapter 11). (Here “meromorphic” means also that the function has a finite number of poles/zeros.) This field consists of all rational functions of x . Denote this field by \mathbf{K}_0 .

Consider the field of functions meromorphic on \mathbf{R} , i. e. on the Riemann surface of the function $\Xi(x)$ or of $\Upsilon(x)$. Denote this field by \mathbf{K}_1 . Note that we specify the field by indicating a Riemann surface on which its elements are meromorphic. One can prove a nontrivial theorem that all elements of \mathbf{K}_1 are rational functions of x and $\Upsilon(x)$, so \mathbf{K}_1 is an extension of \mathbf{K}_0 by a single element $\Upsilon(x)$. \mathbf{K}_1 is an *algebraic extension* of \mathbf{K}_0 since the function $\Upsilon(x)$ obeys an algebraic equation with coefficients belonging to \mathbf{K}_0 :

$$\Upsilon^2(x) - (x - \eta_{1,1})(x - \eta_{1,2})(x - \eta_{2,1})(x - \eta_{2,2}) = 0. \tag{32}$$

The fields of functions meromorphic on certain Riemann surfaces are studied in more details, for example, in the monograph [4].

One can prove (see [3], chapter 23) that such an algebraic extension has a *basis*, i. e. a set $\Omega_{1:0} = [\omega_1, \dots, \omega_j]$ of elements of \mathbf{K}_1 such that any element z of \mathbf{K}_1 can be uniquely represented as

$$z(\hat{x}) = q_1(x)\omega_1(\hat{x}) + \dots + q_j(x)\omega_j(\hat{x}), \tag{33}$$

where $q_j \in \mathbf{K}_0$, i. e. they are rational functions of x . A basis of the extension \mathbf{K}_1 over \mathbf{K}_0 can be easily found:

$$\Omega_{1:0} = [1, \Upsilon(\hat{x})]. \tag{34}$$

In other words, the following statement is valid: any function meromorphic on \mathbf{R} can be represented uniquely in the form

$$q(\hat{x}) = z_1(x) + z_2(x)\Upsilon(\hat{x}), \quad z_1, z_2 \in \mathbf{K}_0. \quad (35)$$

The number of elements of the basis is referred to as the *degree* of extension of \mathbf{K}_1 over \mathbf{K}_0 . This degree is equal to 2.

According to the functional problem for the Sommerfed's transformant $A(\tilde{x})$, this transformant should belong to the set of functions meromorphic on \mathbf{R}_3 . This set is also a field. Denote it by \mathbf{K}_3 . As it can be proven (see the next subsection), \mathbf{K}_3 is an algebraic extension of \mathbf{K}_1 , and the degree of the extension is equal to 3. Since $\mathbf{K}_0 \subset \mathbf{K}_3$, one of the elements of the basis can be taken equal to 1. Thus, we are looking for three-valued functions $F_1(\hat{x})$, $F_2(\hat{x})$ (or, the same, six-valued functions $F_1(x)$ and $F_2(x)$) such that

$$\Omega_{3:1} = [1, F_1, F_2] \quad (36)$$

is the basis of \mathbf{K}_3 over \mathbf{K}_1 . The Sommerfeld transformant of the field $A(\tilde{x})$ should be uniquely represented as

$$A(\tilde{x}) = q_0(\hat{x}) + q_1(\hat{x})F_1(\tilde{x}) + q_2(\hat{x})F_2(\tilde{x}), \quad (37)$$

where $q_j(\hat{x})$ belong to \mathbf{K}_1 being rational functions of x and $\Upsilon(\hat{x})$.

Finding the functions $F_1(\tilde{x})$ and $F_2(\tilde{x})$ is an unusual problem since no function whose Riemann surface is \mathbf{R}_3 is given *a priori*. Finding the coefficients of $q_j(x)$ is, conversely, an almost trivial task when the basis (36) is built. They are constructed by using the knowledge of poles and residues of the Sommerfeld transformant, i. e. by using the condition 3 imposed on A .

Note that the concept of a pole / zero at some point on the complex manifolds \mathbf{R} or on \mathbf{R}_3 differs from that on $\overline{\mathbb{C}}$ if the affix of the point is equal to any of the branch points $\eta_{j,l}$. Consider a function $f(\hat{x}) \in \mathbf{K}_1$ such that $f(\eta_{j,l}) = 0$ or $f(\eta_{j,l}) = \infty$. To find the multiplicity of the zero / pole at $\eta_{j,l}$ one should introduce the local variable τ in the neighborhood of $\eta_{j,l}$ in such a way that the neighborhood of $\eta_{j,l}$ on \mathbf{R} is described by a small circle in the τ -plane in a topologically trivial way, i. e. such that $\hat{x}(\tau)$ is a bijection. One can use for example

$$\tau = \sqrt{x - \eta_{j,l}}$$

as such a variable (another choice is to take $\tau = \Upsilon(\hat{x})$). Then, one should express locally $f(\hat{x})$ in terms of τ , i. e. build a function

$$\theta(\tau) = f(\hat{x}(\tau)).$$

The multiplicity of zero / pole of f is, by definition, the multiplicity of corresponding zero / pole of $\theta(\tau)$.

For example, the function $\Upsilon(\hat{x})$ has simple zeros on \mathbf{R} at each of the points $\eta_{j,l}$, although it may seem surprising. Moreover, the function

$$\frac{1}{\Upsilon^2(\hat{x})} = \frac{1}{(x - \eta_{1,1})(x - \eta_{2,1})(x - \eta_{1,2})(x - \eta_{2,2})}$$

has double poles at each $\eta_{j,l}$ on \mathbf{R} , while the same function, but considered on \mathbb{C} , has simple poles at those points.

The poles / zeros on \mathbf{R}_3 are defined in the same way as for \mathbf{R} .

For all three surfaces $\overline{\mathbb{C}}$, \mathbf{R} , and \mathbf{R}_3 , the poles / zeros at the infinity can be studied by introducing the local variable $\tau = 1/x$.

The plan for building the function $A(\tilde{x})$ is as follows. First, we construct the functions $F_1(\tilde{x})$, $F_2(\tilde{x})$ and form the basis $\Omega_{3:1}$ (see (36)). Second, we find the coefficients $q_0(\hat{x})$, $q_1(\hat{x})$, $q_2(\hat{x})$ of (37).

Remark

In [1] we studied functions meromorphic on a two-sheets covering of \mathbf{R} , namely on \mathbf{R}_2 . The functions meromorphic on this surface form a field \mathbf{K}_2 . This field can be considered as an extension over \mathbf{K}_1 of degree 2. The basis of this extension is

$$\Omega_{2:1} = [1, Q(x)], \quad Q(x) = \sqrt{(x - \eta_{1,1})(x - \eta_{1,2})}. \quad (38)$$

The field \mathbf{K}_2 can be also considered as an extension over \mathbf{K}_0 . In this case, the basis consist of four elements listed in [1], (50), (51):

$$\Omega_{2:0} = [1, \Upsilon(x), Q(x), Q(x)\Upsilon(x)]. \quad (39)$$

In this case, the coefficients should belong to \mathbf{K}_0 .

3.3 The structure of extension \mathbf{K}_3 over \mathbf{K}_1

According to the standard argument of Galois theory [4], the symmetries of \mathbf{R}_3 are linked with the structure of the field \mathbf{K}_3 . Let us sketch out the proof that the degree of the the extension \mathbf{K}_3 over \mathbf{K}_1 is equal to 3 and that this extension is algebraic.

Let a function $g(\tilde{x}) \in \mathbf{K}_3$ have the property $g(\Lambda(\tilde{x})) = g(\tilde{x})$. Then this function is single-valued on \mathbf{R}_1 , and, thus, $g \in \mathbf{K}_1$.

Consider any function $f(\hat{x})$ meromorphic on \mathbf{R}_3 but not meromorphic on \mathbf{R} . This means that $f \in \mathbf{K}_3$ is not single-valued on \mathbf{R} . Consider the combinations similar to (29), (30), (31):

$$f_0(\tilde{x}) = \frac{1}{3} (f(\hat{x}) + f(\Lambda(\hat{x})) + f(\Lambda(\Lambda(\hat{x})))), \quad (40)$$

$$f_1(\tilde{x}) = \frac{1}{3} (f(\hat{x}) + \varpi^{-1}f(\Lambda(\hat{x})) + \varpi f(\Lambda(\Lambda(\hat{x})))), \quad (41)$$

$$f_2(\tilde{x}) = \frac{1}{3} (f(\hat{x}) + \varpi f(\Lambda(\hat{x})) + \varpi^{-1}f(\Lambda(\Lambda(\hat{x})))), \quad (42)$$

Obviously, if f_0 , f_1 , f_2 are known, the function f can be reconstructed by

$$f(\tilde{x}) = f_0(\tilde{x}) + f_1(\tilde{x}) + f_2(\tilde{x}). \quad (43)$$

Note that

$$f_0(\Lambda(\tilde{x})) = f_0(\tilde{x}), \quad f_1(\Lambda(\tilde{x})) = \varpi f_1(\tilde{x}), \quad f_2(\Lambda(\tilde{x})) = \varpi^{-1} f_2(\tilde{x}). \quad (44)$$

One can conclude from (44) that the functions $f_0, (f_1)^3, (f_2)^3$ are single-valued on \mathbf{R} , and thus belong to \mathbf{K}_1 , i. e. they are represented by (35). Obviously, functions f_1 and f_2 obey cubic equations with coefficients from \mathbf{K}_1 .

Take the basis

$$\Omega_{3:1} = [1, f_1, f_2]. \quad (45)$$

The function f is represented through this basis by using the coefficients $f_0, 1, 1$. Let us show that any other function $f'(\tilde{x}) \in \mathbf{K}_3$ can be represented as (37) using the basis (45). Perform the same procedure as above. Get the functions f'_0, f'_1, f'_2 having the properties (44). Function f'_0 belongs to \mathbf{K}_1 and can be used as the first coefficient of the expansion. Consider the functions $f'_j/f_j(x)$, $j = 1, 2$. They are meromorphic and single-valued on \mathbf{R} , thus they belong to \mathbf{K}_1 . These functions can be used as corresponding coefficients.

4 Finding the basis functions F_1, F_2

4.1 Abelian integral of the first kind on \mathbf{D}_1

As a tool, we use the Abelian integral of the first kind on \mathbf{R} . The detailed description of this subject can be found, e.g., in [3], chapter 12. Since \mathbf{R} is a torus, there is one Abelian integral regular everywhere (up to a constant factor and a constant additive term):

$$\chi(\hat{x}) = \int_{\eta_{2,1}}^{\hat{x}} \frac{dx'}{\Upsilon(\hat{x}')} \quad (46)$$

The integral is assumed to be taken along some contour γ drawn on \mathbf{R} . The contour starts at $\eta_{2,1}$ and ends at some point $\hat{x} \in \mathbf{R}$. Indeed, the starting point is arbitrary, and the value $\eta_{2,1}$ is chosen for convenience. The value of the integral depends not only on the point \hat{x} , but also on the homotopic class of the contour γ .

Consider the contours σ_α and σ_β on \mathbf{R} (see Fig. 4). These contours have a common point $\eta_{2,1}$. Being cut along the contours σ_α and σ_β , the surface \mathbf{R} becomes (topologically) a parallelogram.

Contours σ_α and σ_β play an important role in [1] and here. The contour σ_α is homotopic to the “real waves” contour on \mathbf{R} . This contour is a set of points \hat{x} such that an expression $x^m \Xi^n(\hat{x})$ can be treated as a usual plane wave on the discrete plane. The real waves can be easily defined if $\text{Im}[K] = 0$: they possess $(x, y = \Xi(\hat{x}))$ with $|x| = |y| = 1$ (such waves do not decay in any direction). Thus, the real waves line is composed of two copies of an arc of the unit circle connecting $\eta_{2,1}$ and $\eta_{1,1}$. It is shown in Fig. 5 by a dashed line.

If $\text{Im}[K] \neq 0$, the definition of the real wave may be ambiguous since all waves possess decay / growth in some directions. We fix “real waves” as the connected set of points $(x, y) \in \mathbf{D}$

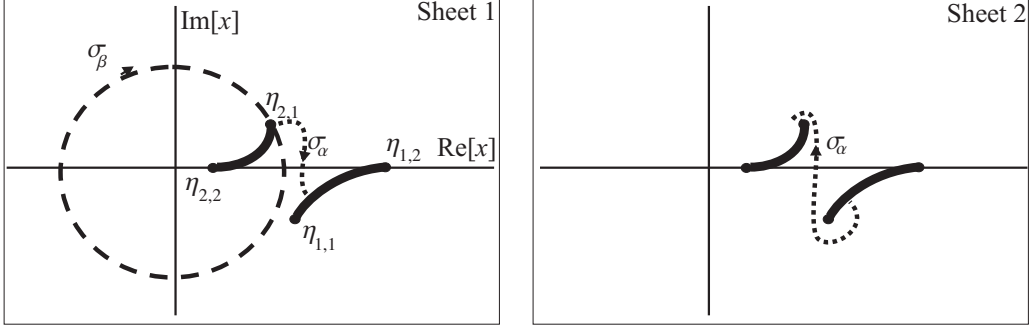


Fig. 4: Contours σ_α and σ_β on \mathbf{R}

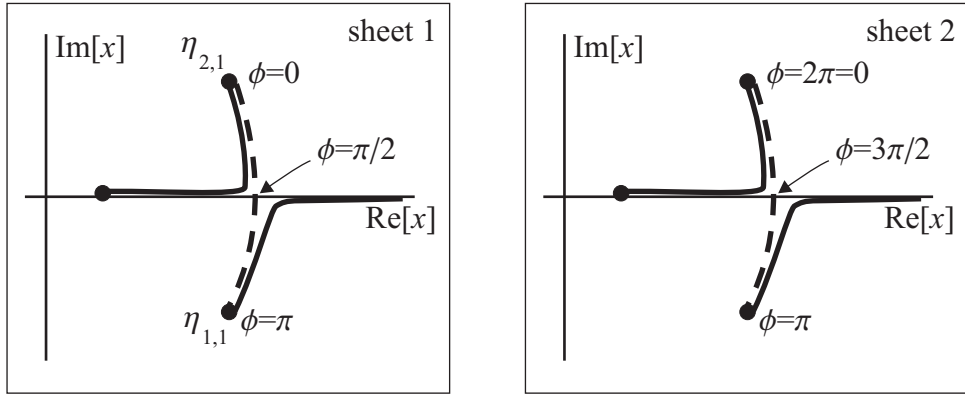


Fig. 5: “Real waves” line on \mathbf{R} for real K (dashed line)

obeying the property

$$\text{Im} \left[\frac{y - y^{-1}}{x - x^{-1}} \right] = 0 \quad (47)$$

and passing through the branch points $\eta_{2,1}$ and $\eta_{1,1}$. This set tends to the line shown in Fig. 5 as $\text{Im}[K] \rightarrow 0$. One can show, e. g. numerically or asymptotically, that the set of all such “real waves” is a closed contour on \mathbf{R} homotopic to σ_α .

The contour σ_β is homotopic to the unit circle on the physical sheet of \mathbf{R} . Being equipped with an orientation, it becomes the integral path for the Green’s function of a discrete plane (see [1]).

Comparing Fig. 4 with Fig. 3 one can conclude that the covering \mathbf{R}_3 of \mathbf{R} is such that the preimage of σ_β is a set of three copies of σ_β , while the preimage of σ_α is a three-sheet covering of σ_α . Note that a bypass along the contour σ_α , being elevated onto \mathbf{R}_3 , changes the sheets of \mathbf{R}_3 cyclically according to the transformation Λ introduced above.

The integrals of the form (46) taken along the closed contours σ_α and σ_β on \mathbf{R} are the *periods* of $\chi(\hat{x})$ referred to as T_α and T_β :

$$T_\alpha = \int_{\sigma_\alpha} \frac{dx}{\Upsilon(\hat{x})}, \quad T_\beta = \int_{\sigma_\beta} \frac{dx}{\Upsilon(\hat{x})}. \quad (48)$$

The mapping $\hat{x} \rightarrow \chi$ maps the surface \mathbf{R} cut along the contours σ_α and σ_β onto an elementary parallelogram in the complex χ -plane. This parallelogram is shown in Fig. 6, left.

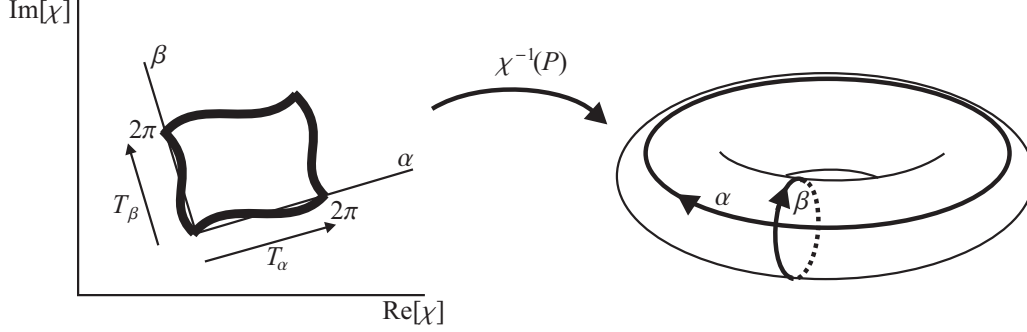


Fig. 6: Elementary parallelogram in the χ -plane and coordinates (α, β) on a torus

Consider an inverse mapping $\psi : \chi \rightarrow \hat{x}$. As it is known, this mapping has the following properties:

$$\psi(\chi + T_\alpha) = \psi(\chi + T_\beta) = \psi(\chi), \quad (49)$$

i. e. it is bi-periodic. This property can be used for introduction of coordinates α and β on \mathbf{R} , revealing the structure of \mathbf{R} as the structure of a torus. Namely, the coordinates α and β can be introduced as linear combinations

$$\alpha = c_{1,1}\text{Re}[\chi] + c_{1,2}\text{Im}[\chi], \quad \beta = c_{2,1}\text{Re}[\chi] + c_{2,2}\text{Im}[\chi], \quad (50)$$

with the coefficients $c_{j,k}$ found from the following equations

$$c_{1,1}\text{Re}[T_\alpha] + c_{1,2}\text{Im}[T_\alpha] = 2\pi, \quad c_{1,1}\text{Re}[T_\beta] + c_{1,2}\text{Im}[T_\beta] = 0, \quad (51)$$

$$c_{2,1}\text{Re}[T_\alpha] + c_{2,2}\text{Im}[T_\alpha] = 0, \quad c_{2,1}\text{Re}[T_\beta] + c_{2,2}\text{Im}[T_\beta] = 2\pi. \quad (52)$$

The coordinates (α, β) on \mathbf{R} are shown in Fig. 6, right. The surface \mathbf{R} is displayed schematically as a torus, i. e. \mathbf{R} is deformed in an appropriate way. The resulting surface is compact, thus, the infinities are represented as two points on it. The coordinate lines of α and β on the initial representation of \mathbf{R} are close² to those shown in Fig. 4 of [1].

According to the schemes in Fig. 2 and Fig. 3, the torus \mathbf{R} corresponds to the parallelogram

$$\mathbf{R} : \quad 0 \leq \alpha < 2\pi, \quad 0 \leq \beta < 2\pi,$$

while the torus \mathbf{R}_3 corresponds to the parallelogram

$$\mathbf{R}_3 : \quad 0 \leq \alpha < 6\pi, \quad 0 \leq \beta < 2\pi.$$

² Coordinates α and β are close to the coordinates α and β defined in [1], but not exactly the same. Note that the requirement that $\beta = \pi$ on the “real waves” line is not fulfilled in the new formulation.

Each point $(\alpha, \beta) \in \mathbf{R}$ is the image of three points $(\alpha, \beta), (\alpha + 2\pi, \beta), (\alpha + 4\pi, \beta)$ of the covering \mathbf{R}_3 .

The symmetries Λ and Π have the following representations in the coordinates (α, β) :

$$\begin{aligned}\Lambda : \quad \alpha &\rightarrow \alpha + 2\pi, & \beta &\rightarrow \beta, \\ \Pi : \quad \alpha &\rightarrow 4\pi - \alpha, & \beta &\rightarrow -\beta.\end{aligned}$$

4.2 Elementary meromorphic functions on the torus \mathbf{R}

We are starting with an auxiliary problem. For any 4 points $\hat{a}_1, \hat{a}_2, \hat{b}_1, \hat{b}_2$ on \mathbf{R} find out whether there exists a function $M(\hat{x}) \in \mathbf{K}_1$ having simple poles \hat{b}_1, \hat{b}_2 only, and simple zeros \hat{a}_1, \hat{a}_2 only, and, indeed, build such a function if it exists.

A criterion of existence of such a function M is known. This criterion is the Abel's theorem (see [5], chapter 10) : On \mathbf{R} , there should exist a contour γ_1 going from \hat{a}_1 to \hat{b}_1 and a contour γ_2 going from \hat{a}_2 to \hat{b}_2 such that

$$\int_{\gamma_1} \frac{dx}{\Upsilon(\hat{x})} + \int_{\gamma_2} \frac{dx}{\Upsilon(\hat{x})} = 0. \quad (53)$$

The criterion has a transcendent (non-algebraic) character. In this subsection we are going to derive an algebraic version of it.

A general case

Assume that a_1, a_2, b_1, b_2 are all distinct values not equal to infinity or to $\eta_{j,l}$. This is the general case. Some important particular cases will be considered below.

Let us try to construct function $M(\hat{x})$ explicitly. First, construct function $M(\hat{x})$ (possibly depending on parameters) having poles at \hat{b}_1 and \hat{b}_2 . An obvious Ansatz (up to a common constant factor) is as follows:

$$M(\hat{x}) = \frac{\Upsilon(\hat{x})}{(x - b_1)(x - b_2)} + \frac{g_1}{x - b_1} + \frac{g_2}{x - b_2} + c. \quad (54)$$

for some complex values g_1, g_2, c . As above, x, a_1, a_2, b_1, b_2 are the affixes of the points $\hat{x}, \hat{a}_1, \hat{a}_2, \hat{b}_1, \hat{b}_2$, respectively.

For arbitrary g_1, g_2 , this function has poles at four points of \mathbf{R} : at $P_{1:0}^{-1}(b_1)$ and $P_{1:0}^{-1}(b_2)$. Choose the values of g_1, g_2 such that they suppress the poles that have affixes b_1, b_2 , but that are not \hat{b}_1 and \hat{b}_2 . One can see that the appropriate function is as follows:

$$M(\hat{x}) = \frac{\Upsilon(\hat{x})}{(x - b_1)(x - b_2)} + \frac{\Upsilon(\hat{b}_1)}{(x - b_1)(b_1 - b_2)} + \frac{\Upsilon(\hat{b}_2)}{(x - b_2)(b_2 - b_1)} + c. \quad (55)$$

Now let us fix the zeros. Choose parameter c in such a way that $M(\hat{a}_1) = 0$:

$$c = - \left[\frac{\Upsilon(\hat{a}_1)}{(a_1 - b_1)(a_1 - b_2)} + \frac{\Upsilon(\hat{b}_1)}{(a_1 - b_1)(b_1 - b_2)} + \frac{\Upsilon(\hat{b}_2)}{(a_1 - b_2)(b_2 - b_1)} \right]. \quad (56)$$

Finally, the condition guaranteeing that \hat{a}_2 is also a zero is the equation

$$\frac{\Upsilon(\hat{a}_2)}{(a_2 - b_1)(a_2 - b_2)} + \frac{\Upsilon(\hat{b}_1)}{(a_2 - b_1)(b_1 - b_2)} + \frac{\Upsilon(\hat{b}_2)}{(a_2 - b_2)(b_2 - b_1)} = \frac{\Upsilon(\hat{a}_1)}{(a_1 - b_1)(a_1 - b_2)} + \frac{\Upsilon(\hat{b}_1)}{(a_1 - b_1)(b_1 - b_2)} + \frac{\Upsilon(\hat{b}_2)}{(a_1 - b_2)(b_2 - b_1)}. \quad (57)$$

This is an equation linking $\hat{a}_1, \hat{a}_2, \hat{b}_1, \hat{b}_2$ that guarantees existence of a function $M(\hat{x})$ meromorphic on \mathbf{R} , having simple zeros at \hat{a}_1, \hat{a}_2 and simple poles at \hat{b}_1, \hat{b}_2 . Thus, (57) is an algebraic analog of the analytic equation (53). The function M itself is given by (55), (56).

Another (more symmetrical) form of (57) is

$$(b_1 - b_2)[(a_1 - b_1)(a_1 - b_2) \Upsilon(\hat{a}_2) - (a_2 - b_1)(a_2 - b_2) \Upsilon(\hat{a}_1)] = (a_1 - a_2)[(a_1 - b_1)(a_2 - b_1) \Upsilon(\hat{b}_2) - (a_1 - b_2)(a_2 - b_2) \Upsilon(\hat{b}_1)]. \quad (58)$$

A special case: poles \hat{b}_1 and \hat{b}_2 coincide

The coincidence of \hat{b}_1 and \hat{b}_2 means that $\hat{b} = \hat{b}_1 = \hat{b}_2$ is a pole of order 2. The Ansatz for M that should replace (55) is as follows:

$$M(\hat{x}) = \frac{\Upsilon(\hat{x})}{(x - b)^2} + \frac{\Upsilon(\hat{b})}{(x - b)^2} + \frac{\dot{\Upsilon}(\hat{b})}{x - b} + c, \quad (59)$$

where

$$\dot{\Upsilon}(\hat{x}) \equiv \frac{d\Upsilon(\hat{x})}{dx}. \quad (60)$$

The constant c is chosen in such a way that $M(\hat{a}_1) = 0$:

$$c = - \left[\frac{\Upsilon(\hat{a}_1)}{(a_1 - b)^2} + \frac{\Upsilon(\hat{b})}{(a_1 - b)^2} + \frac{\dot{\Upsilon}(\hat{b})}{a_1 - b} \right] \quad (61)$$

Finally, this function is zero at \hat{a}_1 if

$$\frac{\Upsilon(\hat{a}_1)}{(a_1 - b)^2} + \frac{\Upsilon(\hat{b})}{(a_1 - b)^2} + \frac{\dot{\Upsilon}(\hat{b})}{a_1 - b} = \frac{\Upsilon(\hat{a}_2)}{(a_2 - b)^2} + \frac{\Upsilon(\hat{b})}{(a_2 - b)^2} + \frac{\dot{\Upsilon}(\hat{b})}{a_2 - b}. \quad (62)$$

Thus, (62) is the condition of existence of a meromorphic function on \mathbf{R} having zeros at \hat{a}_1 and \hat{a}_2 , and a double pole at \hat{b} . The same condition should be valid for existence of a function with a double zero at \hat{b} and simple poles at \hat{a}_1 and \hat{a}_2 .

A special case: poles \hat{b}_1 and \hat{b}_2 coincide with a branch point $\eta_{j,l}$

If \hat{a}_1 and \hat{a}_2 are different points of \mathbf{R} having the same (arbitrary) affix $a_1 = a_2 = a$, then no condition is needed. One can draw the contours γ_1 and γ_2 on different sheets of \mathbf{R} such that

$P_{1:0}(\gamma_1) = P_{1:0}(\gamma_2)$, and (53) will be valid automatically. The function $M(\hat{x})$ is then as follows:

$$M(\hat{x}) = \frac{x - a}{x - \eta_{j,l}}. \quad (63)$$

Note that $\eta_{j,l}$ is a double pole of M on \mathbf{R} according to a comment at the end of Section 3.

A detailed study based on the bijection between the elementary parallelogram in the χ -plane and \mathbf{R} shows that if \hat{a}_1 and \hat{a}_2 have different affixes, a corresponding function M cannot exist.

A special case: a double pole at \hat{b}_1 , a simple zero at \hat{b}_2 , another simple zero at $\eta_{j,l}$, affixes of \hat{b}_1 and \hat{b}_2 coincide: $b_1 = b_2 = b$

A function with a double pole at \hat{b}_1 and regular at \hat{b}_2 is as follows:

$$M(\hat{x}) = \frac{\Upsilon(\hat{x})}{(x - b)^2} + \frac{\Upsilon(\hat{b}_1)}{(x - b)^2} + \frac{\dot{\Upsilon}(\hat{b}_1)}{x - b} + c. \quad (64)$$

Function $M(\hat{x})$ has a zero at \hat{b}_2 if

$$c = \frac{\ddot{\Upsilon}(\hat{b}_1)}{2}, \quad (65)$$

where

$$\ddot{\Upsilon}(\hat{x}) \equiv \frac{d^2 \Upsilon(\hat{x})}{dx^2}.$$

Since $\Upsilon(\eta_{j,l}) = 0$, the condition $M(\eta_{j,l}) = 0$ reads as

$$\frac{\Upsilon(\hat{b}_1)}{(\eta_{j,l} - b)^2} + \frac{\dot{\Upsilon}(\hat{b}_1)}{\eta_{j,l} - b} + \frac{\ddot{\Upsilon}(\hat{b}_1)}{2} = 0. \quad (66)$$

Indeed, equations (62) and (66) are also algebraic versions of (53) in the corresponding special cases.

4.3 Building the elements F_1 and F_2 of the basis $\Omega_{3:1}$

In this subsection we describe the main result of the paper, namely, we build functions F_1 and F_2 .

The difficulty of building the basis $\Omega_{3:1}$ is as follows. The reasoning made above shows that constructing of, say, $F_1(\tilde{x})$ should include taking a cubic radical of a function belonging to \mathbf{K}_1 . Let this function be $G(\hat{x})$, i. e. let be

$$F_1(\tilde{x}) = G^{1/3}(\hat{x}). \quad (67)$$

Since function F_1 is not allowed to have branch points on \mathbf{R} , all poles and zeros of $G(\hat{x})$ on \mathbf{R} should have order 3ν , $\nu \in \mathbb{Z}$. At the same time, if function $G(\hat{x})$ is a cube of another function from \mathbf{K}_1 , say

$$G(\hat{x}) = g^3(\hat{x}),$$

then the values of $G^{1/3}(\hat{x})$ are just $g(\hat{x})$, $\varpi g(\hat{x})$, $\varpi^{-1}g(\hat{x})$. All of these functions belong to \mathbf{K}_1 , and thus, cannot contribute to a basis $\Omega_{3:1}$. Therefore, it is necessary to find a function $G(\hat{x}) \in \mathbf{K}_1$, having poles and zeros of order 3ν , but that is not a cube of a function from \mathbf{K}_1 .

Remark.

This can be illustrated by the example solved in [1], where a basis $\Omega_{2:1}$ has been constructed. A non-trivial element of this basis is $Q(x)$ defined by (38). One can see that

$$Q(x) = G_2^{1/2}(x),$$

where

$$G_2(x) = (x - \eta_{1,1})(x - \eta_{1,2}),$$

The function G_2 has double zeros at $x = \eta_{1,1}$ and $x = \eta_{1,2}$ (they are double in the sense of local variable τ on the complex manifold \mathbf{R} , see above), and two double poles at the infinities of the two sheets of \mathbf{R} . However, $G_2(x)$ is not a square of any function meromorphic on \mathbf{R} .

To get $F_1(\hat{x})$ having the Riemann surface \mathbf{R}_3 , one should impose two additional restrictions on $G(\hat{x})$. Namely, the variation of the argument of G along σ_β should be equal to $6\pi\nu$, $\nu \in \mathbb{Z}$, while its variation along σ_α should be $2\pi(3\nu + 1)$ or $2\pi(3\nu + 2)$.

Let us describe the procedure of constructing the function $G(\hat{x})$. First, we describe it in terms of the Abel's criterion. Consider the period T_β defined by (48). Take an arbitrary point $\hat{a} \in \mathbf{R}$. Find the points \hat{b}, \hat{c} on \mathbf{R} such that

$$\int_{\gamma_1} \frac{dx}{\Upsilon(x)} = \int_{\gamma_2} \frac{dx}{\Upsilon(x)} = \int_{\gamma_3} \frac{dx}{\Upsilon(x)} = \frac{T_\beta}{3}. \quad (68)$$

The contours $\gamma_{1,2,3}$ cyclically connecting the points $\hat{a}, \hat{b}, \hat{c}$ are shown in Fig. 7, right. The Riemann surface \mathbf{R} is shown schematically as a torus in this figure, i. e. it is deformed homotopically to emphasize its topology. The contours σ_α and σ_β introduced by Fig. 4 are shown in Fig. 7, left. We take the contours $\gamma_1, \gamma_2, \gamma_3$ such that their concatenation is homotopic to σ_β .

To find such points, \hat{b}, \hat{c} , one can build explicitly the coordinate line $\alpha = \text{const}$ starting from \hat{a} , i. e. the line along which the integral

$$\int_{\hat{a}}^{\hat{x}} \frac{dx'}{\Upsilon(\hat{x}')}$$

changes linearly from 0 to T_β . Then one should split this segment into 3 equal parts in the χ -plane. Contours $\gamma_1, \gamma_2, \gamma_3$ can be taken as corresponding straight segments in the χ -plane subject to the mapping ψ .

Construct two functions $M_1(\hat{x})$ and $M_2(\hat{x})$ such that:

- M_1 has a double pole at \hat{a} and simple zeros at \hat{b} and \hat{c} ;
- M_2 has a double pole at \hat{b} and simple zeros at \hat{a} and \hat{c} .

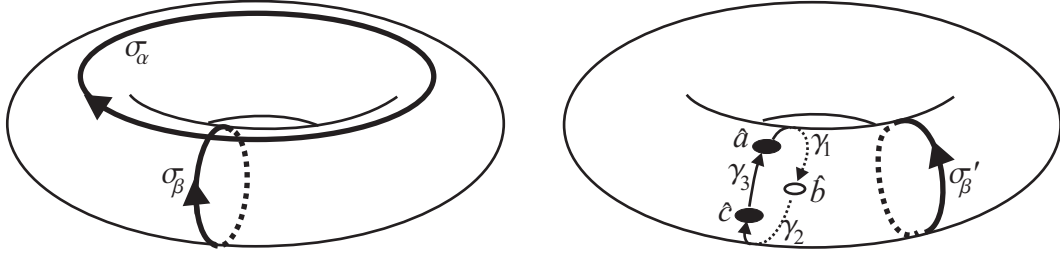


Fig. 7: Contours σ_α and σ_β on \mathbf{R} (left). Points \hat{a} , \hat{b} , \hat{c} on the torus \mathbf{R} (right)

Both functions do exist according to the Abel's criterion.

Function G is constructed as

$$G(\hat{x}) = \frac{M_1(\hat{x})}{M_2(\hat{x})}. \quad (69)$$

By construction, $G(\hat{x})$ has a triple pole at \hat{a} and a triple zero at \hat{b} . There are no other poles or zeros of G .

Function F_1 defined by (67) is three-valued on \mathbf{R}_1 and has no branch points. Moreover, the F_1 cannot be a meromorphic function on \mathbf{R}_1 , since there is no function meromorphic on \mathbf{R}_1 and having a single simple pole / zero on it.

Let us find the change of the argument of the function $G(\hat{x})$ along the contour σ_β . Compute the phase change on the contour σ'_β shown in Fig. 7, right, not passing through the points \hat{a} , \hat{b} , \hat{c} , and taken parallel to the β -axis in the (α, β) -plane. What is important, this contour goes not cross the contours $\gamma_1, \gamma_2, \gamma_3$ since they are taken also parallel to the β -axis by construction.

Consider a family of functions $M(\hat{z}_1; \hat{x})$ (\hat{x} is considered as an argument and \hat{z}_1 is a parameter, both belong to \mathbf{D}_1). The functions are as follows. Construct points z_2 and z_3 in such a way that

$$\int_{\hat{z}_1}^{\hat{z}_2} \frac{dx}{\Upsilon(x)} = \int_{\hat{z}_2}^{\hat{z}_3} \frac{dx}{\Upsilon(x)} = \int_{\hat{z}_3}^{\hat{z}_1} \frac{dx}{\Upsilon(x)} = \frac{T_\beta}{3}. \quad (70)$$

and demand that $M(\hat{z}_1; \hat{x})$ has a double pole at \hat{z}_1 and simple zeros in \hat{z}_2 and \hat{z}_3 . Normalize M in any invariant way (say, by the residue of M^{-1} at \hat{z}_2). By construction, the family $M(\hat{z}_1; \hat{x})$ is continuous with respect to \hat{z}_1 . Moreover,

$$M_1(\hat{x}) = M(\hat{a}; \hat{x}), \quad M_2(\hat{x}) = M(\hat{b}; \hat{x}).$$

Carry \hat{z}_1 from \hat{a} to \hat{b} continuously along γ_1 . The argument variation of $M(\hat{z}; \hat{x})$ is continuous during this change (since the points $\hat{z}_1, \hat{z}_2, \hat{z}_3$ do not hit the contour σ'_β), thus this argument variation remains constant. Therefore the phase change of G on σ'_β is zero.

Homotopic deformation of σ'_β into some σ''_β may lead to the crossing of a triple zero or a triple pole of G , thus the argument variation of G along σ''_β is $3\pi\nu$ for some $\nu \in \mathbb{Z}$. The parameter ν depends on the particular choice of σ_β .

A similar but slightly more complicated consideration can be applied to computation of the argument variation of G along σ_α . Consider the crossing of the contours σ_α and σ_β . The pair of the coordinate vectors $(\mathbf{e}_\alpha, \mathbf{e}_\beta)$, being considered on the local complex coordinate plane τ is oriented as the pair $(\text{Im}[\tau], \text{Re}[\tau])$, and this fact is a topological invariant, i. e. it remains unchanged with any homotopic deformation of σ_α and σ_β leaving their intersection transversal. One can show that in this case the argument variation of G along σ_α is $2\pi(3\nu + 1)$, $\nu \in \mathbb{Z}$. The parameter ν depends on the particular choice of σ_α .

Fix the point \hat{a} as $\eta_{2,1}$ for simplicity. Then the points \hat{b} and \hat{c} should have the same affix, still unknown (see the second special case in the previous subsection). Denote corresponding point \hat{b} by $\hat{\mathbf{b}}$ and its affix by \mathbf{b} . This point plays an important role in what follows. Denote the point \hat{c} having the same affix \mathbf{b} , but located on another sheet of \mathbf{R} , by $\hat{\mathbf{c}}$.

Function M_1 is given by the formula (63):

$$M_1(\hat{x}) = \frac{x - \mathbf{b}}{x - \eta_{2,1}}. \quad (71)$$

Function $M_2(\hat{x})$ is constructed in (64), (65):

$$M_2(\hat{x}) = \frac{\Upsilon(\hat{x})}{(x - \mathbf{b})^2} + \frac{\Upsilon(\hat{\mathbf{b}})}{(x - \mathbf{b})^2} + \frac{\dot{\Upsilon}(\hat{\mathbf{b}})}{x - \mathbf{b}} + \frac{\ddot{\Upsilon}(\hat{\mathbf{b}})}{2} \quad (72)$$

provided that equation (66) is valid for $\hat{b}_1 = \hat{\mathbf{b}}$ and $\eta_{j,l} = \eta_{2,1}$. We discuss finding of $\hat{\mathbf{b}}$ in details in the next subsection.

Thus, when the point $\hat{\mathbf{b}}$ is found, the function $F_1(\tilde{x})$ can be written as:

$$F_1(\tilde{x}) = \left(\frac{\Upsilon(\hat{x})}{(x - \mathbf{b})^2} + \frac{\Upsilon(\hat{\mathbf{b}})}{(x - \mathbf{b})^2} + \frac{\dot{\Upsilon}(\hat{\mathbf{b}})}{x - \mathbf{b}} + \frac{\ddot{\Upsilon}(\hat{\mathbf{b}})}{2} \right)^{-1/3} \left(\frac{x - \mathbf{b}}{x - \eta_{2,1}} \right)^{1/3}. \quad (73)$$

Note that the function F_1 is defined by (73) ambiguously. This ambiguity follows from that of the cubic radical, i. e. the result can be multiplied by ϖ or ϖ^{-1} . This ambiguity is partly addressed below.

Let us list the properties of the function $F_1(\tilde{x})$:

- It has Riemann surface \mathbf{R}_3 .
- It has simple poles at three points of \mathbf{R}_3 having affixes $\eta_{2,1}$. There are no other poles (including infinities).
- It has simple zeros at three points of \mathbf{R}_3 that are $P_{3,1}^{-1}(\hat{\mathbf{b}})$. There are no other zeros (including infinities).
- As it follows from the argument change of G along σ_α ,

$$F_1(\Lambda(\tilde{x})) = \varpi F_1(\tilde{x}). \quad (74)$$

Let us build the function F_2 . Note that

$$\Upsilon(\hat{\mathbf{c}}) = -\Upsilon(\hat{\mathbf{b}}), \quad \dot{\Upsilon}(\hat{\mathbf{c}}) = -\dot{\Upsilon}(\hat{\mathbf{b}}), \quad \ddot{\Upsilon}(\hat{\mathbf{c}}) = -\ddot{\Upsilon}(\hat{\mathbf{b}}).$$

Construct a function $M_3(\hat{x})$ having a double pole at $\hat{\mathbf{c}}$ and simple zeros at $\eta_{2,1}$ and at $\hat{\mathbf{b}}$. Then take

$$F_2(\tilde{x}) = (M_1(\hat{x})/M_3(\hat{x}))^{1/3}. \quad (75)$$

Similarly to (73),

$$F_2(\tilde{x}) = \left(-\frac{\Upsilon(\hat{x})}{(x-\mathbf{b})^2} + \frac{\Upsilon(\hat{\mathbf{b}})}{(x-\mathbf{b})^2} + \frac{\dot{\Upsilon}(\hat{\mathbf{b}})}{x-\mathbf{b}} + \frac{\ddot{\Upsilon}(\hat{\mathbf{b}})}{2} \right)^{-1/3} \left(\frac{x-\mathbf{b}}{x-\eta_{2,1}} \right)^{1/3}. \quad (76)$$

The properties of $F_2(\tilde{x})$ are as follows:

- It has Riemann surface \mathbf{R}_3 .
- It has simple poles at three points of \mathbf{R}_3 having affixes $\eta_{2,1}$. There are no other poles (including the infinities).
- It has simple zeros at three points of \mathbf{R}_3 that are $P_{3:1}^{-1}(\hat{\mathbf{c}})$. The affixes of these points are equal to \mathbf{b} . There are no other zeros (including the infinities).
- Similarly to F_1 ,

$$F_2(\Lambda(\tilde{x})) = \varpi^{-1} F_2(\tilde{x}). \quad (77)$$

This property of F_2 and the similar property of F_1 guarantee that the elements of the basis (36) are linearly independent.

Besides, there are some properties linking F_1 and F_2 .

The symmetry Π converts F_1 into F_2 :

$$F_1(\Pi(\tilde{x})) = \delta F_2(\tilde{x}), \quad \delta \in \{1, \varpi, \varpi^{-1}\}. \quad (78)$$

To prove this, use (24) and note that

$$\frac{\Upsilon(\hat{x})}{(x-\mathbf{b})^2} + \frac{\Upsilon(\hat{\mathbf{b}})}{(x-\mathbf{b})^2} + \frac{\dot{\Upsilon}(\hat{\mathbf{b}})}{x-\mathbf{b}} + \frac{\ddot{\Upsilon}(\hat{\mathbf{b}})}{2} \xrightarrow{\Pi} -\frac{\Upsilon(\hat{x})}{(x-\mathbf{b})^2} + \frac{\Upsilon(\hat{\mathbf{b}})}{(x-\mathbf{b})^2} + \frac{\dot{\Upsilon}(\hat{\mathbf{b}})}{x-\mathbf{b}} + \frac{\ddot{\Upsilon}(\hat{\mathbf{b}})}{2}$$

To remove some of the ambiguity of determining F_1 and F_2 , fix the value $\delta = 1$, thus fixing

$$F_1(\Pi(\tilde{x})) = F_2(\tilde{x}). \quad (79)$$

The product of functions F_1 and F_2 is rational. Namely, it belongs to \mathbf{K}_1 since

$$F_1(\Lambda(\tilde{x}))F_2(\Lambda(\tilde{x})) = F_1(\tilde{x})F_2(\tilde{x}),$$

and, then, it belongs to \mathbf{K}_0 since

$$F_1(\Pi(\tilde{x}))F_2(\Pi(\tilde{x})) = F_1(\tilde{x})F_2(\tilde{x}).$$

One can easily see that $F_1(\tilde{x})F_2(\tilde{x})$ should have a simple pole at $x = \eta_{2,1}$ and a simple zero at $x = \mathbf{b}$. Studying the function at infinity, one can find that

$$F_1(\tilde{x})F_2(\tilde{x}) = \frac{1}{((\ddot{\Upsilon}(\hat{\mathbf{b}}))^2/4 - 1)^{1/3}} \frac{x - \mathbf{b}}{x - \eta_{2,1}}. \quad (80)$$

Indeed, some ambiguity is still left in the choice of the branch of the cubic root. This ambiguity, however, does not affect the final formulae.

4.4 Algebraic equations for finding the affix \mathbf{b}

Here our aim is to replace the transcendent equation (68) by an algebraic equation. As before, we consider a special case when $\hat{a} = \eta_{2,1}$.

Let us use the condition (65) of existence of a function M_2 having a double pole at $\hat{\mathbf{b}}$ and simple zeros $\eta_{2,1}$ and $\hat{\mathbf{c}}$, provided that $\hat{\mathbf{b}}$ and $\hat{\mathbf{c}}$ have the same affix \mathbf{b} :

$$\frac{\Upsilon(\hat{\mathbf{b}})}{(\eta_{2,1} - \mathbf{b})^2} + \frac{\dot{\Upsilon}(\hat{\mathbf{b}})}{\eta_{2,1} - \mathbf{b}} + \frac{\ddot{\Upsilon}(\hat{\mathbf{b}})}{2} = 0. \quad (81)$$

Note that ratios $\dot{\Upsilon}(\hat{\mathbf{b}})/\Upsilon(\hat{\mathbf{b}})$ and $\ddot{\Upsilon}(\hat{\mathbf{b}})/\Upsilon(\hat{\mathbf{b}})$ are rational functions of \mathbf{b} . Thus, (81) is an algebraic equation for \mathbf{b} . After some algebra, equation (81) becomes reduced to the fourth order equation:

$$h_0 + h_1\mathbf{b} + h_2\mathbf{b}^2 + h_3\mathbf{b}^3 + h_4\mathbf{b}^4 = 0, \quad (82)$$

where

$$\begin{aligned} h_0 &= \eta_{2,1} + 3\eta_{1,2} - \eta_{2,1}^2\eta_{1,2} + \eta_{2,1}\eta_{1,2}^2, \\ h_1 &= -4(1 + 2\eta_{2,1}\eta_{1,2} + \eta_{1,2}^2), \\ h_2 &= 6(\eta_{2,1} + \eta_{1,2} + \eta_{2,1}^2\eta_{1,2} + \eta_{2,1}\eta_{1,2}^2), \\ h_3 &= -4\eta_{2,1}(\eta_{2,1} + 2\eta_{1,2} + \eta_{2,1}\eta_{1,2}^2), \\ h_4 &= \eta_{2,1} - \eta_{1,2} + 3\eta_{2,1}^2\eta_{1,2} + \eta_{2,1}\eta_{1,2}^2. \end{aligned}$$

The algebraic condition (82) is slightly weaker than the transcendent condition (70). Namely, equation (82) is fulfilled if there exist *any* contours $\gamma_1, \gamma_2, \gamma_3$ cyclically connecting the points $\eta_{2,1}$ and two points on \mathbf{R} having affix \mathbf{b} , such that

$$\int_{\gamma_1} \frac{dx}{\Upsilon(\hat{x})} = \int_{\gamma_2} \frac{dx}{\Upsilon(\hat{x})} = \int_{\gamma_3} \frac{dx}{\Upsilon(\hat{x})}. \quad (83)$$

The concatenation of the contours $\gamma_1 + \gamma_2 + \gamma_3$ is not necessarily homotopic to σ_β , thus, each of the integrals is not necessarily equal to $T_\beta/3$.

A detailed study shows that the equation (82) has four roots: b_1, b_2, b_3, b_4 , such that

$$\int_{\eta_{2,1}}^{b_1} \frac{dx}{\Upsilon(\hat{x})} = \pm \frac{T_\beta}{3} + \mu T_\beta + \nu T_\alpha, \quad (84)$$

$$\int_{\eta_{2,1}}^{b_2} \frac{dx}{\Upsilon(\hat{x})} = \pm \frac{T_\alpha}{3} + \mu T_\beta + \nu T_\alpha, \quad (85)$$

$$\int_{\eta_{2,1}}^{b_3} \frac{dx}{\Upsilon(\hat{x})} = \pm \frac{T_\alpha + T_\beta}{3} + \mu T_\beta + \nu T_\alpha, \quad (86)$$

$$\int_{\eta_{2,1}}^{b_4} \frac{dx}{\Upsilon(\hat{x})} = \pm \frac{T_\alpha - T_\beta}{3} + \mu T_\beta + \nu T_\alpha. \quad (87)$$

The integrals are defined up to the sign and up to the integers μ, ν , which depend on the particular choice of the integration contour. One can see that only b_1 fits the condition (70), i. e. $\mathbf{b} = b_1$.

For practical computations, we propose two following algorithms for computing the value \mathbf{b} with a high accuracy.

Algorithm 1:

1. Compute T_β by numerical integration.
2. Find \mathbf{b} approximately from the condition

$$\int_{\eta_{2,1}}^{\mathbf{b}} \frac{dx}{\Upsilon(x)} = \frac{T_\beta}{3}. \quad (88)$$

For this, solve numerically the ordinary differential equation

$$\frac{dx}{d\chi} = \Upsilon(x) \quad (89)$$

on the segment $\chi \in [0, T_\beta/3]$. Take $x(0) = \eta_{2,1}$. The value $x(T_\beta/3)$ is the approximation for \mathbf{b} . Denote it by \mathbf{b}' .

3. Using \mathbf{b}' as a starting approximation, solve (82) by Newton's method. As a result, after several iterations, get a refined value of \mathbf{b} .

Since the first two steps are necessary only to obtain the starting approximation for Newton's method used on the third step, very coarse meshes can be used for numerical integration and for solving the ordinary differential equation. The Newton's method is very cheap, and, several iterations provide the value of \mathbf{b} having the machine accuracy.

Another algorithm can be developed, taking the algebraic equation (82) as the starting point. The algorithm is as follows.

Algorithm 2:

1. Solve equation (82) and find four values: b_1, b_2, b_3, b_4 .
2. For each value b_j construct the function $G(\hat{x})$ by (69) and check the variation of $\text{Arg}[G]$ along the contour σ_β . There should exist only one value of \mathbf{b} (among the four values found on step 1), for which the variation of $\text{Arg}[G]$ is equal to zero. This value of \mathbf{b} is what we are looking for.

Indeed, Algorithm 1 and Algorithm 2 should yield the same result.

Remark

To solve the ordinary differential equation (89) near the branch point $\eta_{2,1}$ one can use the local variable on \mathbf{R} , namely,

$$\tau = \tau(x) = \sqrt{x - \eta_{2,1}}.$$

One can rewrite (89) as an ODE for $\tau(\chi)$:

$$\frac{d\tau}{d\chi} = \frac{1}{2} \sqrt{(\tau^2 + \eta_{2,1} - \eta_{1,1})(\tau^2 + \eta_{2,1} - \eta_{1,2})(\tau^2 + \eta_{2,1} - \eta_{2,2})} \left(= \frac{\Upsilon}{2\tau} \right). \quad (90)$$

Thus, one can solve (90) in some small neighborhood of $\eta_{2,1}$, and then solve (89).

5 Constructing the Sommerfeld transformant $A(x)$

Here we assume that x_{in} and x_{in}^{-1} are not equal to \mathbf{b} or to $\eta_{j,l}$.

Let us build the Sommerfeld transformant $A(\tilde{x})$ obeying the functional problem formulated in Subsection 2.1. For this, we use the representation (37) expressing A through the basis $\Omega_{3;1}$. The functions F_1 and F_2 are built above.

The coefficients $q_j(\hat{x})$ of the representation (37) belong to \mathbf{K}_1 . Thus,

$$q_j(\hat{x}) = q'_j(x) + q''_j(x)\Upsilon(\hat{x}), \quad j = 0, 1, 2, \quad (91)$$

where $q'_j(x)$ and $q''_j(x)$ belong to \mathbf{K}_0 , i. e. they are rational functions. The aim of this section is to find the functions $q'_j(x)$ and $q''_j(x)$.

According to the representation (26) with properties (27) and (74), (77),

$$A_0(\tilde{x}) = q'_0(x) + q''_0(x)\Upsilon(\hat{x}), \quad (92)$$

$$A_1(\tilde{x}) = (q'_1(x) + q''_1(x)\Upsilon(\hat{x}))F_1(\tilde{x}), \quad (93)$$

$$A_2(\tilde{x}) = (q'_2(x) + q''_2(x)\Upsilon(\hat{x}))F_2(\tilde{x}). \quad (94)$$

To build the functions $q'_j(x)$ and $q''_j(x)$, one should study poles and zeros of these functions. Let us formulate a series of statements.

1. Let x_0 be not equal to ∞ , $\eta_{j,l}$, \mathbf{b} , x_{in} , or x_{in}^{-1} . Then all functions $q'_j(x)$, $q''_j(x)$, $j = 0, 1, 2$ are regular at x_0 .

The proof is as follows. Consider some particular j . Let ν be the highest pole order of the functions $q'_j(x)$, $q''_j(x)$ at x . Note that $F_{1,2}(x_0) \neq 0$ and $\Upsilon(x_0) \neq 0$. Thus, the pole of order ν will appear on the sheet 1 or 2 (corresponding residues cannot be compensated both). This contradicts to the functional problem for A_j .

The statements 2, 3 and 4 are similar to statement 1, so we omit their proofs.

2. The functions $q'_k(x)$, $q''_k(x)$, $k = 0, 1, 2$ are regular at the points $\eta_{1,1}$, $\eta_{1,2}$, $\eta_{2,2}$.

3. The functions $q'_k(x)$, $x^2q''_k(x)$, $k = 0, 1, 2$ are regular at infinity.

4. The functions $q'_k(x)$, $q''_k(x)$ have simple poles at x_{in} and x_{in}^{-1} .

Slightly more subtle consideration is needed for the values x equal to $\eta_{2,1}$ and \mathbf{b} , since functions F_1 and F_2 have poles and zeros at these affixes. The following statements can be proven:

5. The functions $q'_0(x)$, $q''_0(x)$, $(x - \eta_{2,1})^{-1}q'_1(x)$, $q''_1(x)$, $(x - \eta_{2,1})^{-1}q'_2(x)$, $q''_2(x)$ are regular at $x = \eta_{2,1}$.

6. Functions q'_0 and q''_0 are regular at \mathbf{b} . $q'_j(x)$, $q''_j(x)$, $j = 1, 2$ can have simple poles at \mathbf{b} . The following identities should be valid:

$$\lim_{x \rightarrow \mathbf{b}} [q'_1(x) - \Upsilon(\hat{\mathbf{b}})q''_1(x)] = 0, \quad \lim_{x \rightarrow \mathbf{b}} [q'_2(x) + \Upsilon(\hat{\mathbf{b}})q''_2(x)] = 0,$$

Using these statements, one can find the most general form for the functions $q'_j(x)$, $q''_j(x)$ obeying statements 1–6:

$$q'_0(x) = \frac{s_1}{x - x_{\text{in}}} + \frac{s_2}{x - x_{\text{in}}^{-1}} + s_0, \quad (95)$$

$$q''_0(x) = \frac{s_3}{x - x_{\text{in}}} - \frac{s_3}{x - x_{\text{in}}^{-1}}, \quad (96)$$

$$q'_1(x) = (x - \eta_{2,1}) \left(\frac{s_4}{x - x_{\text{in}}} + \frac{s_5}{x - x_{\text{in}}^{-1}} - \frac{(s_6 + s_7)\Upsilon(\hat{\mathbf{b}})}{x - \mathbf{b}} \right), \quad (97)$$

$$q''_1(x) = (\mathbf{b} - \eta_{2,1}) \left(\frac{s_6}{x - x_{\text{in}}} + \frac{s_7}{x - x_{\text{in}}^{-1}} - \frac{s_6 + s_7}{x - \mathbf{b}} \right), \quad (98)$$

$$q_2'(x) = (x - \eta_{2,1}) \left(\frac{s_8}{x - x_{\text{in}}} + \frac{s_9}{x - x_{\text{in}}^{-1}} + \frac{(s_{10} + s_{11})\Upsilon(\hat{\mathbf{b}})}{x - \mathbf{b}} \right), \quad (99)$$

$$q_2''(x) = (\mathbf{b} - \eta_{2,1}) \left(\frac{s_{10}}{x - x_{\text{in}}} + \frac{s_{11}}{x - x_{\text{in}}^{-1}} - \frac{s_{10} + s_{11}}{x - \mathbf{b}} \right). \quad (100)$$

One can see that these functions contain 12 scalar parameters s_0, \dots, s_{11} . The parameter s_0 can be chosen arbitrarily (we assume further that $s_0 = 0$). The rest 11 parameters can be found from the known residues of A_j at $\tilde{x}_1, \tilde{x}_2, \tilde{x}_3, \tilde{x}_4$.

Using these residues given by the formulation of the functional problems for $A_j(\tilde{x})$, build a system of equations for s_1, \dots, s_{11} :

$$s_1 = iY_1/(6\pi), \quad s_2 = iY_3/(6\pi), \quad s_3 = 0, \quad (101)$$

$$(x_{\text{in}} - \eta_{2,1})s_4F_1(\tilde{x}_1) + (b - \eta_{2,1})s_6Y_1F_1(\tilde{x}_1) = iY_1/(6\pi), \quad (102)$$

$$(x_{\text{in}} - \eta_{2,1})s_4F_1(\tilde{x}_2) - (b - \eta_{2,1})s_6Y_1F_1(\tilde{x}_2) = iY_1/(6\pi), \quad (103)$$

$$(x_{\text{in}} - \eta_{2,1})s_8F_2(\tilde{x}_1) + (b - \eta_{2,1})s_{10}Y_1F_2(\tilde{x}_1) = iY_1/(6\pi), \quad (104)$$

$$(x_{\text{in}} - \eta_{2,1})s_8F_2(\tilde{x}_2) - (b - \eta_{2,1})s_{10}Y_1F_2(\tilde{x}_2) = iY_1/(6\pi), \quad (105)$$

$$(x_{\text{in}}^{-1} - \eta_{2,1})s_5F_1(\tilde{x}_3) + (b - \eta_{2,1})s_7Y_3F_1(\tilde{x}_3) = iY_3/(6\pi), \quad (106)$$

$$(x_{\text{in}}^{-1} - \eta_{2,1})s_5F_1(\tilde{x}_4) - (b - \eta_{2,1})s_7Y_3F_1(\tilde{x}_4) = iY_3/(6\pi), \quad (107)$$

$$(x_{\text{in}}^{-1} - \eta_{2,1})s_9F_2(\tilde{x}_3) + (b - \eta_{2,1})s_{11}Y_3F_2(\tilde{x}_3) = iY_3/(6\pi), \quad (108)$$

$$(x_{\text{in}}^{-1} - \eta_{2,1})s_9F_2(\tilde{x}_4) - (b - \eta_{2,1})s_{11}Y_3F_2(\tilde{x}_4) = iY_3/(6\pi). \quad (109)$$

The equations (102)–(109) can be easily solved. The result can be written using (80) as follows:

$$s_4 = Z\Upsilon(\hat{x}_1) \frac{1}{x_{\text{in}} - \mathbf{b}} (F_2(\tilde{x}_1) + F_2(\tilde{x}_2)), \quad (110)$$

$$s_6 = Z \left(\frac{1}{\mathbf{b} - \eta_{2,1}} + \frac{1}{x_{\text{in}} - \mathbf{b}} \right) (F_2(\tilde{x}_1) - F_2(\tilde{x}_2)), \quad (111)$$

$$s_8 = Z\Upsilon(\hat{x}_1) \frac{1}{x_{\text{in}} - \mathbf{b}} (F_1(\tilde{x}_1) + F_1(\tilde{x}_2)), \quad (112)$$

$$s_{10} = Z \left(\frac{1}{\mathbf{b} - \eta_{2,1}} + \frac{1}{x_{\text{in}} - \mathbf{b}} \right) (F_1(\tilde{x}_1) - F_1(\tilde{x}_2)), \quad (113)$$

$$s_5 = Z \Upsilon(\hat{x}_3) \frac{1}{x_{\text{in}}^{-1} - \mathbf{b}} (F_2(\tilde{x}_3) + F_2(\tilde{x}_4)), \quad (114)$$

$$s_7 = Z \left(\frac{1}{\mathbf{b} - \eta_{2,1}} + \frac{1}{x_{\text{in}}^{-1} - \mathbf{b}} \right) (F_2(\tilde{x}_3) - F_2(\tilde{x}_4)), \quad (115)$$

$$s_9 = Z \Upsilon(\hat{x}_3) \frac{1}{x_{\text{in}}^{-1} - \mathbf{b}} (F_1(\tilde{x}_3) + F_1(\tilde{x}_4)), \quad (116)$$

$$s_{11} = Z \left(\frac{1}{\mathbf{b} - \eta_{2,1}} + \frac{1}{x_{\text{in}}^{-1} - \mathbf{b}} \right) (F_1(\tilde{x}_3) - F_1(\tilde{x}_4)), \quad (117)$$

where

$$Z = \frac{i((\ddot{\Upsilon}(\hat{\mathbf{b}}))^2/4 - 1)^{1/3}}{12\pi}. \quad (118)$$

Finally, the Sommerfeld transformant is found. The formulae that should be used for computations are (26), (92), (93), (94), (101), (110)–(117).

6 Why $u(m, n)$ obeys the diffraction problem?

Here we check directly that the Sommerfeld integral (17) defines the wave $u(m, n)$ obeying all conditions imposed on it.

Consistency of the Sommerfeld integral

One can see that $u(m, n)$ is defined in a different way for the domains $m \leq 0$ and $n \leq 0$, namely the integration contours Γ_2 and Γ_3 are different (see (18), (19)). Let us show that these representations yield the same result in the intersection of the domains, namely, in the quadrant $m \leq 0$ and $n \leq 0$. For this, let us show that

$$\int_{J_3} w_{m,n}(x, \Xi(\hat{x})) A(\tilde{x}) \frac{dx}{\Upsilon(\hat{x})} = \int_{J_3'} w_{m,n}(x, \Xi(\hat{x})) A(\tilde{x}) \frac{dx}{\Upsilon(\hat{x})} = 0 \quad \text{for } m \leq 0 \text{ and } n \leq 0. \quad (119)$$

The proof is straightforward. One can see that at the infinities of the sheets 2 and 4 of the scheme shown in Fig. 3 both x and $\Xi(\hat{x})$ tend to ∞ . Thus, the function $w_{m,n}(x, \Xi(\hat{x}))$ does not grow as $|x| \rightarrow \infty$. According to the conditions imposed on A , the integrals are equal to zero.

Validity of the discrete Helmholtz equation

Substitute the representation (17) with (18) for $m < 0$, or with (19) for $n < 0$. Substitute this representation into the equation (1). Note that the the discrete Laplace operator acts only on w . A direct check shows that (1) is valid.

Radiation condition

Let us demonstrate that $u(m, n)$ obeys the radiation condition formulated in the form of the limiting absorption principle. For this, deform the contours Γ_2 and Γ_3 homotopically as follows:

$$\Gamma_2 = \lambda_1 + \lambda_2 + \lambda_3, \quad \Gamma_3 = \lambda_3 + \lambda_4 + \lambda_5, \quad (120)$$

where contours $\lambda_1, \dots, \lambda_5$ are shown in Fig. 8. Sheets 5 and 6 are not shown. Contours λ_1 and λ_2 are drawn around corresponding cuts (we remind that the cuts are conducted along the sets of x for which $|y(\hat{x})| = 1$). Contours λ_4 and λ_5 are unit circles. Contour λ_3 encircles x_{in} . Note that $|x_{\text{in}}| < 1$.

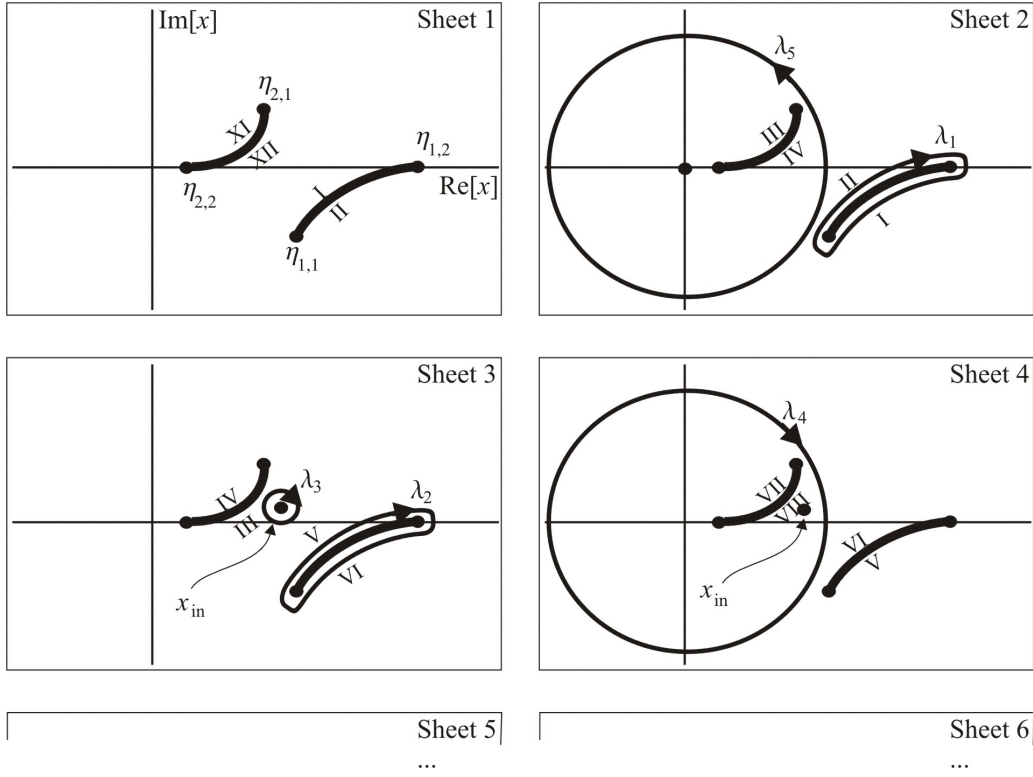


Fig. 8: Contours of integration $\lambda_1, \dots, \lambda_5$

One can see that

$$\int_{\lambda_3} w_{m,n}(\hat{x}, y(\hat{x})) A(\tilde{x}) \frac{dx}{\Upsilon(\hat{x})} = u_{\text{in}}. \quad (121)$$

As the result, the following representations of the field are obtained:

$$u(m, n) = u_{\text{in}}(m, n) + \int_{\lambda_1 + \lambda_2} w_{m,n}(\hat{x}, y(\hat{x})) A(\tilde{x}) \frac{dx}{\Upsilon(\hat{x})} \quad \text{for } m \leq 0, \quad (122)$$

$$u(m, n) = u_{\text{in}}(m, n) + \int_{\lambda_4 + \lambda_5} w_{m,n}(\hat{x}, y(\hat{x})) A(\tilde{x}) \frac{dx}{\Upsilon(\hat{x})} \quad \text{for } n \leq 0. \quad (123)$$

Consider the exponential factor $w_{m,n} = x^m y^n$ of the representation (122). For each point of the representation contours, $|y| = 1$ and $|x| > 1$. Since $m \leq 0$, the result should decay for large negative m . Besides, the field should decay for constant negative m and growing positive n due to the oscillatory nature of factor w on the contours λ_1 and λ_2 .

Similarly, for the representation (123), $|x| = 1$ and $|y| > 1$ in the exponential factor, thus the field should decay for large negative n .

Thus, we obtain that the total field is a sum of the incident field and a decaying field.

Boundary conditions

Let us check the boundary condition $u = 0$ on the side $m \geq 0, n = 0$. For this, use the representation (17), (19).

On the boundary $m \geq 0, n = 0$, the contour of the Sommerfeld integral can be deformed into two unit circles drawn in sheet 3 and 4 (see Fig. 9). Namely,

$$u(m, 0) = \int_{\lambda_4 + \lambda_6} x^m A(\tilde{x}) \frac{dx}{\Upsilon(\tilde{x})}. \quad (124)$$

Due to the symmetry (25), this integral is zero.

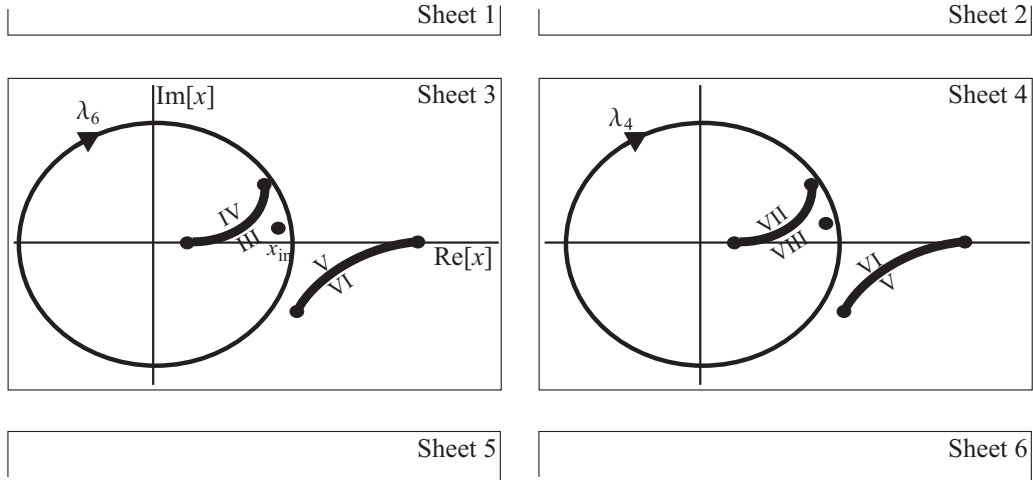


Fig. 9: Contours of integration λ_4 and λ_6

The situation is slightly more subtle with the boundary $m = 0, n \geq 0$. As it follows from the consideration performed in [1], the Sommerfeld integral is introduced invariantly with respect to the choice of the independent variable. For example, one can choose y as an independent variable, and repeat the whole consideration based on this variable. This would lead to an integral representation

$$u(m, n) = - \int_{\Gamma_j} w_{m,n}(\Xi(\hat{y}), y) A'(\hat{y}) \frac{dy}{\Upsilon(\hat{y})}. \quad (125)$$

The new Sommerfeld transformant A' is linked with the old transformant by the relation

$$A'(\hat{y}) = A(\tilde{x}(\hat{y})). \quad (126)$$

Since the whole consideration can be repeated in the variable y , the symmetry argument described here can be also reproduced. The symmetry Π' mentioned above should be used. The axes m and n become swapped, so now this argument works for the boundary $m = 0, n \geq 0$.

7 Numerical examples

In this section we are demonstrating the ideas of the paper using some numerical examples. In all cases we take real values of K , having in mind the limit $\text{Im}[K] \rightarrow +0$.

7.1 Computation of $\hat{\mathbf{b}}$

Take $K = 0.5$ and find the point $\hat{\mathbf{b}}$. Use Algorithm 1 for this. First, find the period T_β (see (48)). For the numerical integration, use contour σ_β shown in Fig. 10, left. The positions of the branch point $\eta_{j,l}$ are shown by stars.

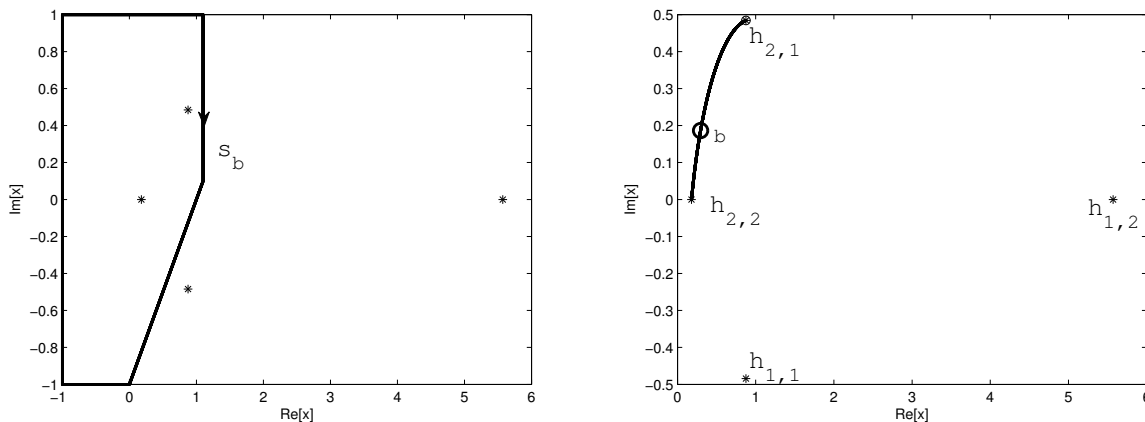


Fig. 10: Contour for finding T_β (left), solution of equation (89), right

Find the correct values of $\Upsilon(\hat{x})$ on this contour. The contour passes through the point $x = 1$ on sheet 1, thus, one can fix $\Upsilon(1)$, and then utilize the continuity. One can see that $\Upsilon(1) = \pm 0.9682i$, and one should choose the correct sign. Take K close to 0.5, but having a small positive imaginary part, say $K = 0.5 + 0.1i$. The values of $\Upsilon(1)$ for this K are $\pm(-0.1810 + 0.9722i)$, and they correspond to the values $y_1 = 0.7895 + 0.4361i$ and $y_2 = 0.9705 - 0.5361i$, respectively. One can see that $|y_1| < 1$ and $|y_2| > 1$. Thus, one should choose $\Upsilon(1) = -0.1810 + 0.9722i$ for $K = 0.5 + 0.1i$. By continuity, $\Upsilon(1) = 0.9682i$ for $K = 0.5$. This reasoning yields that $\text{Im}[\Upsilon(1)] > 0$ on the physical sheet for all real $0 < K < 2$.

The integral for T_β can be easily computed for $K = 0.5$:

$$T_\beta = -1.6219 + 2.4884i.$$

For demonstration purposes, solve the equation (89) (or its equivalent form (90)) on the segment $\chi \in [0, T_\beta]$, taking $x(0) = \eta_{2,1}$. The result is the trajectory going from $\eta_{2,1}$ to $\eta_{2,2}$ along one of the sheets of \mathbf{R} and returning back along another sheet. The trajectory ends almost exactly at $\eta_{2,1}$. The projection of this trajectory onto the x -plane is shown in Fig. 10, right.

According to Algorithm 1, solve equation (89) for $\chi \in [0, T_\beta/3]$, with $x(0) = \eta_{2,1}$. As the result, get the position of the point $\hat{\mathbf{b}}$, i. e. the affix \mathbf{b} and the value $\Upsilon(\hat{\mathbf{b}})$. We use this value as a starting approximation for \mathbf{b} and refer to it as \mathbf{b}' . If the ODE is solved by the simplest Euler's scheme on a mesh of 100 nodes,

$$\mathbf{b}' = 0.2917 + 0.1858i, \quad \Upsilon(\hat{\mathbf{b}}') = -0.2437 + 0.7958i.$$

The position of \mathbf{b}' is shown in Fig. 10, right, by a circle. The value of $\Upsilon(\hat{\mathbf{b}}')$ is needed to conclude that $\hat{\mathbf{b}}'$ belongs to sheet 2 of \mathbf{R} .

The value of \mathbf{b}' obtained so far can be considered as a rough approximation for this parameter. According to Algorithm 1, one can solve (82) by the Newton's method to refine the value. The process stabilizes after 4 steps, and the result is:

$$\mathbf{b} = 0.295390040273516 + 0.186354378894278i.$$

One can see that the starting approximation \mathbf{b}' happens to be quite close to the exact root of (82). This is a clear demonstration of consistency of our approach.

Taking K belonging to a dense grid covering the segment $[10^{-3}, 1]$ and repeating the procedure described above, one can obtain the values $\hat{\mathbf{b}}(K)$. They are presented graphically in Fig. 11. The affix \mathbf{b} is shown by its real and imaginary part. The value $\Upsilon(\hat{\mathbf{b}})$ is necessary only to select a correct sheet of \mathbf{R} , so we displayed the imaginary part of it.

An important conclusion that can be made from Fig. 11 (and of course one can prove this analytically) is that

$$\mathbf{b} \rightarrow 1 \quad \text{as} \quad K \rightarrow 0,$$

and $\hat{\mathbf{b}}$ is located on sheet 2.

7.2 Examination of $G = (F_1)^3$

Fix $K = 0.5$ and use the value of $\hat{\mathbf{b}}$ found in the previous subsection. Let us construct the function $G(\hat{x})$ by the formulae (69), (71), (72), i. e.

$$G(\hat{x}) = \left(\frac{\Upsilon(\hat{x})}{(x - \mathbf{b})^2} + \frac{\Upsilon(\hat{\mathbf{b}})}{(x - \mathbf{b})^2} + \frac{\dot{\Upsilon}(\hat{\mathbf{b}})}{x - \mathbf{b}} + \frac{\ddot{\Upsilon}(\hat{\mathbf{b}})}{2} \right)^{-1} \frac{x - \mathbf{b}}{x - \eta_{2,1}}.$$

Let us check numerically the validity of the non-trivial condition imposed on G , i. e. that the arguments variation of G on σ_β is zero, while the argument variation of G on σ_α is equal to 2π .

To check this, we build hodographs of G on σ_α and on σ_β , i. e. we plot the values of $G(\hat{x})$ for \hat{x} running along the contours σ_α and σ_β . As the result, we get oriented contours in the complex plane of G .

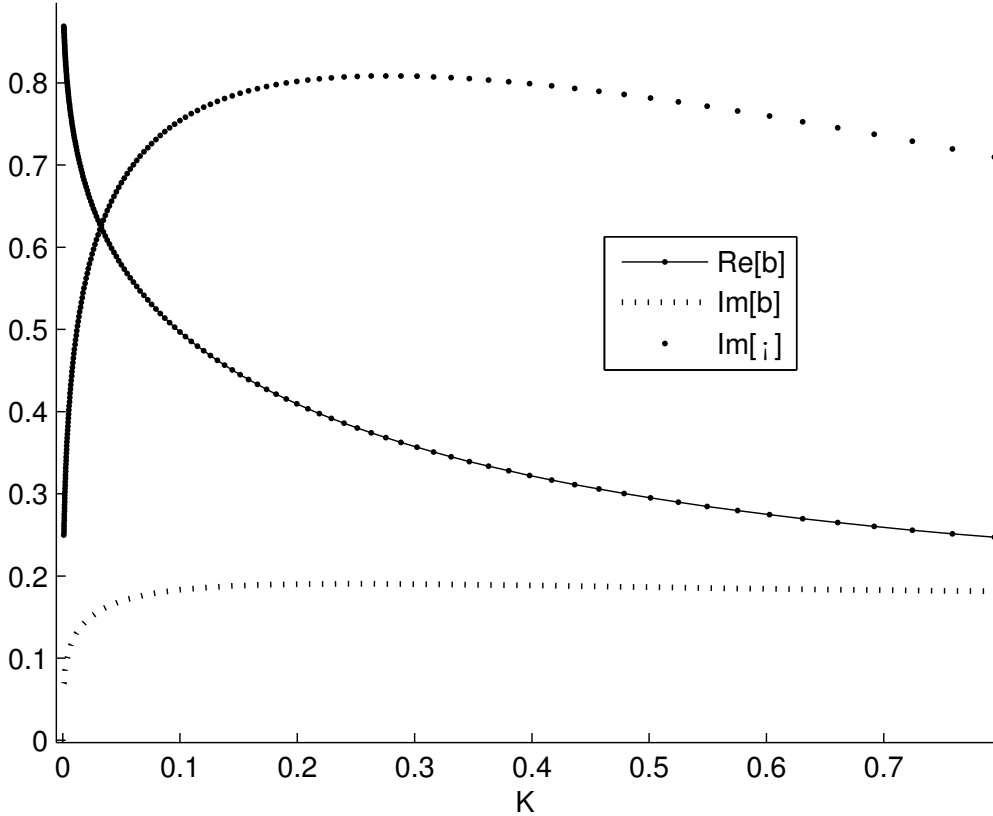


Fig. 11: The values of $\text{Re}[\mathbf{b}]$, $\text{Im}[\mathbf{b}]$, and $\text{Im}[\Upsilon(\hat{\mathbf{b}})]$ as functions of K

The contour homotopic to σ_β has been already built (see Fig. 10, left). The contour homotopic to σ_α and convenient for numerical computations is shown in Fig. 12. The contour passes the value $x = 1$ on sheet 1 on the way down.

The hodographs of $G(\hat{x})$ on σ_α and σ_β are shown in Fig. 13, left and right, respectively. The origin is marked by letter O in both graphs. One can see that the hodograph for σ_α encircles the origin for a single time in the positive direction, and the hodograph for σ_β does not encircle the origin at all. Thus, the conditions for G are valid.

Indeed, a similar check can be performed for $(F_2)^3$.

7.3 Building the wave field $u(m, n)$

Take the value of K equal to 0.5.

For simplicity, we take angle of incidence $\phi_{\text{in}} = \pi/4$. By symmetry, $x_{\text{in}} = y_{\text{in}}$ and we are looking for the solution of the equation $\hat{D}(x_{\text{in}}, x_{\text{in}}) = 0$ corresponding to the wave traveling in

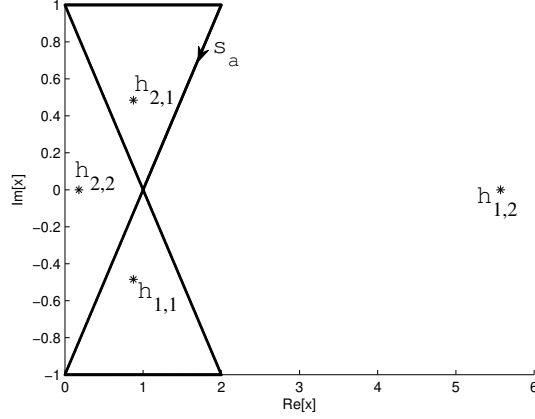


Fig. 12: Contour homotopic to σ_α

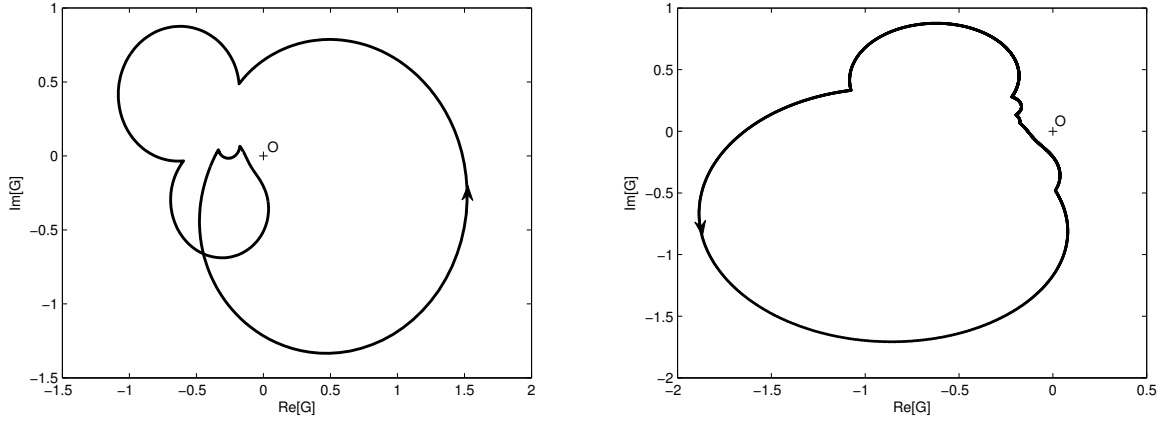


Fig. 13: Hodographs of G on σ_α (left) and on σ_β (right)

the positive direction with respect to m and n :

$$x_{\text{in}} = y_{\text{in}} = \frac{4 - K^2 + iK\sqrt{8 - K^2}}{4} = 0.9375 + 0.3480i.$$

We compute the total field by the formulae (122), (123) with the transformant A represented by (26). The components A_j , $j \in \{0, 1, 2\}$ are computed by (92), (93), (94). We took 50000 nodes on each contour for integration.

The real part of the total field is shown in Fig. 14.

The field pattern corresponds to what can be expected. The field is zero at the boundary, and there are visible zones of the reflected waves.

In Fig. 15 we plot the scattered field u_{sc} only. The real part is in the left, while the imaginary part is in the right. One can see cylindrical wave scattered by the angle vertex.

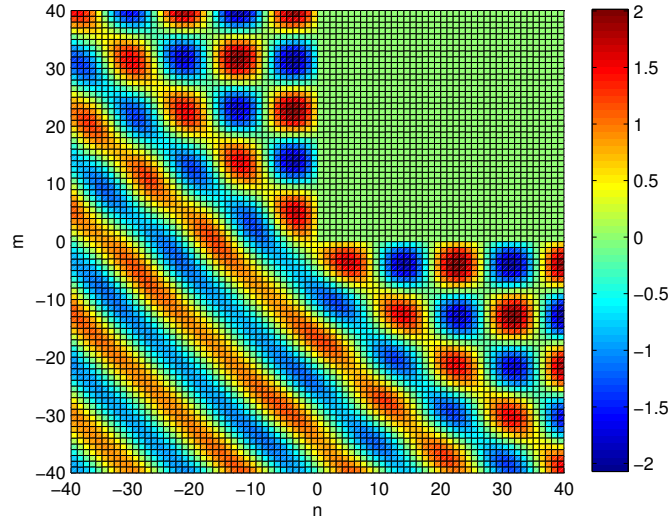


Fig. 14: The real part of $u(m, n)$

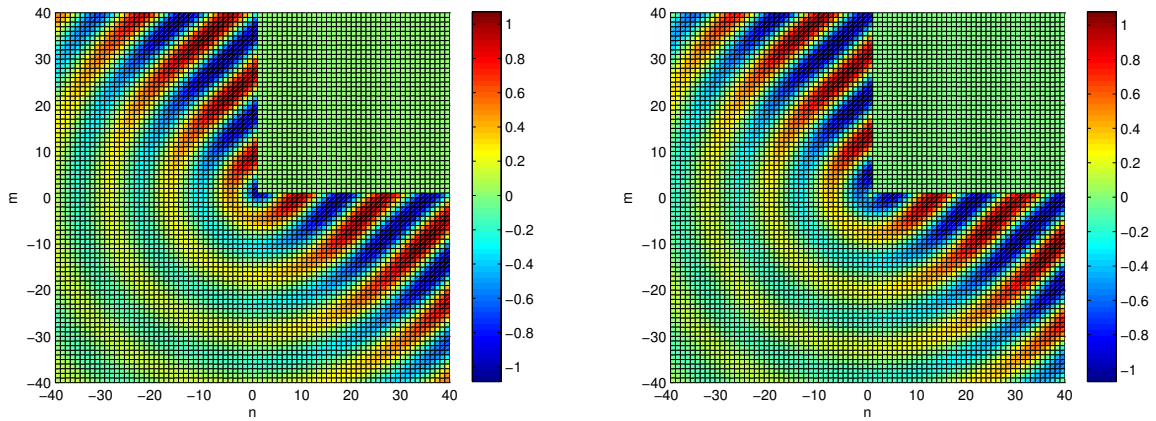


Fig. 15: The scattered wave $u_{sc}(m, n)$. The real part (left); the imaginary part (right)

8 Conclusion

Let us summarize the process of solving the problem of diffraction by a Dirichlet right angle on a discrete plane. Note that the problem is characterized by two parameters: by the wavenumber parameter K of the Helmholtz equation (1) and by the incident angle ϕ_{in} defined by (6). The procedure is as follows:

1. The consideration is based on the structure of the Riemann surface \mathbf{R} . This surface is described by four branch points $\eta_{1,1}, \eta_{1,2}, \eta_{2,1}, \eta_{2,2}$. These branch points depend only on K , and they are found from (12), (13).
2. One should find the period T_β . This can be done by computing the corresponding integral in (48). The contour is shown in Fig. 4, but it is practical to perform the integration along the unit circle in the negative direction. Function $\Upsilon(x)$ is given by the last expression of (14). The branch of $\Upsilon(x)$ is chosen in such a way that $\Xi(x)$ defined by (15) has property $|\Xi(x)| < 1$.
3. The parameter $\hat{\mathbf{b}}$ should be found. This is the point on \mathbf{R} , thus it is characterized by the affix \mathbf{b} and the branch of $\Upsilon(\hat{\mathbf{b}})$.

Algorithm 1 described in Subsection 4.4 can be used for this. According to this algorithm, first, the differential equation (89) is solved numerically on the segment $\chi \in [0, T_\beta/3]$, and an approximation \mathbf{b}' of the parameter \mathbf{b} becomes obtained. Besides, the sheet of \mathbf{R} on which $\hat{\mathbf{b}}$ is located becomes determined. Second, an algebraic equation (82) is solved iteratively using $\hat{\mathbf{b}}'$ as the starting approximation.

4. The functions $F_1(\tilde{x})$ and $F_2(\tilde{x})$ are constructed by (73) and (76). Note that these functions depend on K as on a parameter.
5. The Sommerfeld transformant of the field $A(\tilde{x})$ is built using (26), (92), (93), (94), (101), (110)–(117).
6. The function $u(m, n)$ is built using the Sommerfeld integral (17).

The whole consideration is held in the framework of the Sommerfeld integral. The structure of the integral may seem slightly unusual, however, as we demonstrate in [1], it is a natural generalization of the Sommerfeld integral for angular domains for the discrete case.

We first build the functional field \mathbf{K}_3 to which the Sommerfeld transformant of the field belongs. Note that this field is common for all incident angles. The functional field \mathbf{K}_3 is represented as the basis $\Omega_{3,1}$ composed of three functions or by the basis $\Omega_{3,0}$ composed of six functions. The construction of the basis is a non-trivial procedure. Second, for a particular angle of incidence ϕ_{in} we find the Sommerfeld transformant $A(\tilde{x})$. This task is tedious, but quite simple. The coefficients are rational functions, and one should find these functions obeying some known restrictions and having some known poles. This structure of solution seems to be deeply linked with the embedding procedure [6, 7]. The elements of the basis are either solutions on

the branched physical surface, having some fixed configurations of the incident fields, or they are oversingular solutions. This, possibly, gives a new view on the embedding procedure.

9 Acknowledgements

Authors are grateful to Anastasia Kisil for valuable discussions. The work is supported by the RFBR grant 19-29-06048.

References

- [1] A.V. Shanin and A.I. Korolkov. Sommerfeld-type integrals for discrete diffraction problems. *Wave Motion*, 97:102606, sep 2020.
- [2] B. V. Shabat. *Introduction to complex analysis*. American Mathematical Society, 1992.
- [3] Helmut Koch. *Introduction to Classical Mathematics I : From the Quadratic Reciprocity Law to the Uniformization Theorem*. Springer Netherlands, Dordrecht, 1991.
- [4] Askold Khovanskii. *Topological Galois Theory*. Springer Berlin Heidelberg, 2014.
- [5] George Springer. *Introduction to Riemann surfaces*. American Mathematical Society, Providence, R.I, 2001.
- [6] N. R. T. Biggs. A new family of embedding formulae for diffraction by wedges and polygons. *Wave Motion*, 43(7):517–528, 2006.
- [7] E. A. Skelton, R. V. Craster, and A. V. Shanin. Embedding formulae for diffraction by non-parallel slits. *The Quarterly Journal of Mechanics and Applied Mathematics*, 61(1):93–116, dec 2008.